Thermo-Hydraulic Stability Analysis of the High Performance Light Water Reactor and a Scaled Experimental Facility

M. B. Sanders

Master of Science Thesis

Supervisor:
Dr. M. Rohde

Department of Radiation, Radionuclides and Reactors
Faculty of Applied Sciences
Delft University of Technology

10-08-2009

Abstract

This project uses a code written in COMSOL to investigate the thermo-hydraulic stability of a scaled High Performance Light Water Reactor (HPLWR) and to do an extended parameter study of both the single pass as well as the three pass core design. To this end an existing steady state code was extended to be able find neutral stability boundaries (NSB), simulate different fluids (water and Freon-23) and simulate two new systems (the three pass core and a scaled HPLWR facility (DeLight)).
The code, which is used to search for the NSB's, was validated and its sensitivity to the modeling of the properties of the fluids, as well pressure variations were investigated. By adjusting the properties of Water and Freon-23 the effect of using Freon-23 as a scaling fluid was examined. On top of this the assumptions required for the derivation of the scaling laws for DeLight were examined. Finally a number of parameters of the three pass core HPLWR design were examined to investigate their effect on the stability of the system.
The density should be modelled by a cubic spline based on 30 carefully chosen points and the in- and outlet constrictions should be modeled as part of the core and not as boundary conditions. The NSB of DeLight resembles that of the HPLWR and it can therefore be used to investigate the stability of the HPLWR. The difference in dimensionless density between Freon-23 and water accounts for a large fraction of the difference in stability between the HPLWR and DeLight. The remaining difference can be explained by the assumptions required for the scaling laws. The inertial term had a much greater effect than was expected but this was compensated by an opposite effect due to an approximation of the equation of state. The power distribution in the current three pass core design is, found to be the most destabilising factor and should be adapted.

Contents

Chapter 1

Introduction

1.1 Reducing Oil Dependence and Carbon Emissions

To sustain its present lifestyle mankind consumes large amounts of natural resources. One category of resources have been very useful and therefore extensively consumed: hydrocarbons. Due to our growing demand for energy we have burnt huge amounts of hydrocarbons causing a significant increase in the concentration of carbon-dioxide in our atmosphere. Although it is hard to prove, there are strong indications that this increased level of carbon-dioxide could cause climate change on a global scale. Thus, to prevent the possible disastrous effects of climate change, our energy need must to be supplied by alternative means.
There is another problem: due to the large-scale consumption of hydrocarbons over the past century the depletion of oil and gas reserves is coming into sight. Though there are still large amounts within reach and even more just waiting for the right technology, it is entirely plausible that within the next 50 to 100 years we will have depleted the reserves or are unable to produce enough to satisfy our collective (growing) energy needs.
Furthermore, the dependence of the western world on hydrocarbons and in particular oil causes yet another problem. The main oil reserves in the world are located in politically unstable states or states which are not always on friendly terms with the western world. This leaves the west vulnerable to boycotts such as in 1973.
The dependence on hydrocarbons for our energy provision must be reduced to avoid these problems. Energy sources which do not pollute the environment and cannot be depleted would be the best solution to our predicament. There are however a number of difficulties with the available renewable energy sources: they require enormous amounts of surface area to be able to produce significant amounts of energy and often have to be subsidised to be commercially viable (e.g. wind energy, solar energy and biofuel). Other

options are only useful in specific geographic locations which have the right local topography (e.g. geothermal energy and hydro power). This severely limits the amount of renewable energy which can be supplied and leaves a gap between our energy consumption and the amount of energy which can be supplied by renewable sources.
This leads to an alternative which has been taboo since the early 1980's but has since the start of the new millennium become an increasingly acceptable alternative to hydrocarbons: nuclear energy. Nuclear energy has been taboo for a three of good reasons. There is a risk of proliferation of technology and materials which would enable countries to produce weapons of mass destruction. Nuclear waste: reactors produce long lived radio-active isotopes which remain dangerous for up to 10 000 years. The final major concern regarding nuclear reactors, is the risk of a serious accident or meltdown.
The threat of an accident has been reduced by improving reactor design based on insights gained in research and by experience. Moreover the use of fast reactors could considerably reduce the amount of long lived nuclear waste which would reduce the burden we place on future generations. The creation of geological deposits for nuclear waste such as Olkiluoto in Finland, brings secure storage of long lived nuclear waste within reach and the ever increasing efficiency of nuclear reactors makes them commercially attractive.
Even though the objections raised have only been diminished and not removed, nuclear power will have to form a significant, perhaps even increasing, part of the energy mix which needs to be used to overcome problems regarding climate change and reliability. If and when sufficient amounts of renewable energy are available, nuclear power might be phased out. In the mean while, probably at least till the end of this century, nuclear power needs to be considered as a serious solution to the problems we face regarding our energy supply.

1.2 High Performance Light Water Reactor

The current generation of nuclear power reactors being built are part of the improved generation III reactors and are primarily either boiling water reactors (BWR) or pressurised water reactors (PWR)(see Fig.1.1). The High Performance Light Water Reactor (HPLWR, a European design) or Super Critical Water Reactor (SCWR, an American Design), as it is also known, is a generation IV reactor and is an improvement on the PWR using known supercritical power plant technology. The goal of the HPLWR design is to maximise the theoretical thermodynamic efficiency by increasing the maximum outlet temperature. The outlet temperature in a water cooled reactor is mainly limited by the dual function of water. It not only acts as coolant but also as moderator. If the temperature is raised too high the water no

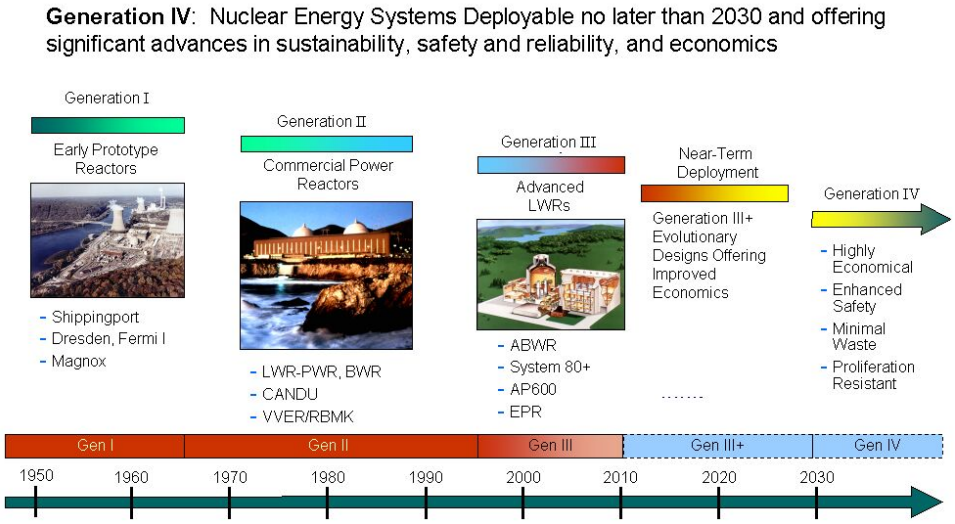

Figure 1.1: Generation IV roadmap [7]

longer has a sufficiently high density to keep on functioning as moderator, thus stopping the fission reaction in the core. To overcome this problem one can raise the operating pressure thereby increasing the temperature at which water boils and allowing for a higher thermodynamic efficiency. This is the operating concept of the PWR. The HPLWR takes this concept a step further by increasing the pressure by a factor 4 allowing a possible $\sim$10% gain in efficiency from 35% to 44% [24]. Furthermore the HPLWR is a much simpler design. Since there are no two phase flows there is no longer a need for steam separators and recirculation pumps, considerably lowering the cost of construction of the nuclear plant.

There are, however, a number of obstacles to be overcome to achieve the highest possible exit enthalpy/temperature. High temperatures decrease the lifespan of elements of the core such as the cladding and reactor pressure vessel (RPV). On top of this, not all channels will have the same temperature and some can become 200°C hotter than the average. These "hot" channels can cause damage to the core. To prevent this the hot channels are mixed with colder channels [23] at the top and bottom of the core. This is achieved by using a three pass core as shown in Fig. 1.2. In the European HPLWR design, the 52 channel clusters of the preceding core section enter the mixing plane and are mixed so that the water enters the next section at a homogeneous temperature, thus avoiding extreme cases of hot channels [23] and achieving an exit temperature of 500°C without reaching the design limit of the cladding material in the hot channel ($620 - 630$°C[23]).

The high exit temperature does have a drawback which lies in the dual function of water as both the cooling liquid and the moderator of the reactor.

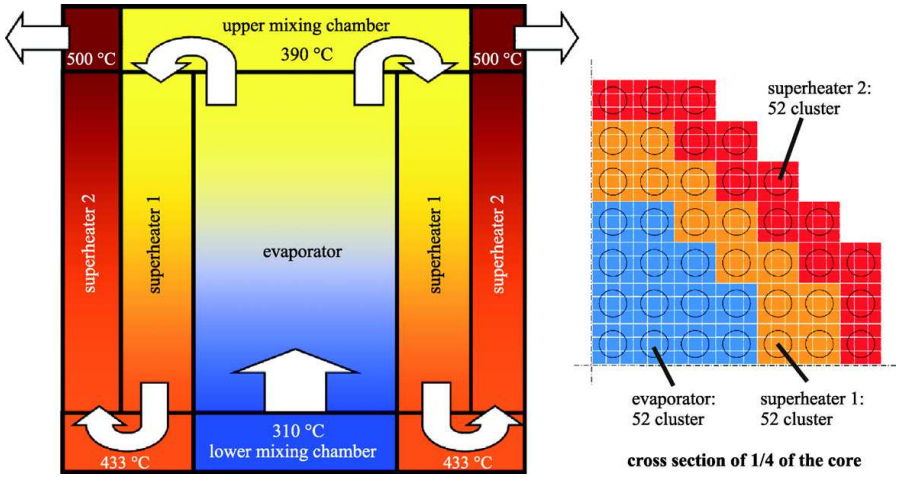

Figure 1.2: On the left a side-view cross section of the three pass core. On the right a top view cross section of the three pass core.[23]

At the exit of the superheater II the water will have a density $100kg.m^{-3}$ or less which impairs its function as moderator and preventing optimal performance. By leading up to 25% [23] of the downcomer water through the core as extra moderator the effects of the low density water at the exit of the core can be compensated.

Under the extreme conditions present in an HPLWR, water is neither in a fluid nor in a gaseous phase. Instead it is said to be supercritical. Above $22MPa$ and 373.9°C water no longer exhibits phase changes. Properties, such as density, now gradually, vary along a range of temperatures. For example, at $25MPa$, the density of water varies from $900kg.m^{-3}$ at 200°C to $100kg.m^{-3}$ at 600°C. Other properties undergo similar gradual changes as can be seen in Fig. 1.3.

Since there is no phase change it is also impossible to establish a boiling boundary or a density linked to the liquid ρ_f or gaseous phase ρ_g, which are necessary to calculate the conventional dimensionless numbers, the subcooling number and phase-change number. The reference point used to scale supercritical fluids is the pseudo-critical point. The pseudo-critical point is the closest thing to a boiling point a supercritical fluid has. To find the pseudo-critical point we use the heat capacity as it exhibits a sharp peak at the pseudo-critical point. Properties of the fluid at the pseudo-critical point will be used throughout the thesis and will be denoted by a subscript $_{pc}$ such as: h_{pc}, ρ_{pc} and μ_{pc}.

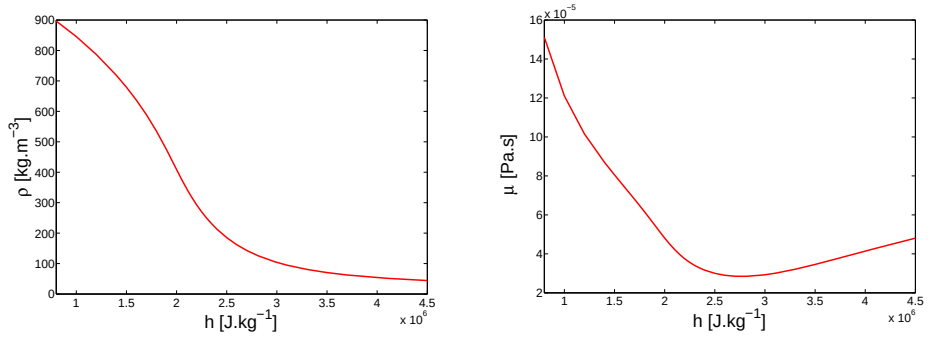

(a) Density of water (b) Viscosity of water

Figure 1.3: Properties of Water as function of enthalpy at the nominal pressure of 25MPa

1.3 Stability

Systems such as the HPLWR can become unstable in certain cases. This implies that perturbations which occur in the system tend to grow causing large variations in a state variable. An example of an unstable system can be seen in Fig.1.4b. In a stable system a perturbation will dampen, as can be seen in Fig.1.4a. By changing a parameter of a system such as power its stability properties can be altered. At certain operating points (i.e. set of parameters defining the system) a stable system will become unstable. This point lies on the neutral stability boundary (NSB). An unstable system is to be avoided and so it is important to know the location of the NSB. Numerically this can be achieved by calculating the eigenvalues of a system linearized at a certain operating point. Depending on the way the eigenvalues are defined either positive or negative eigenvalues represent unstable states. If the negative eigenvalues represent unstable eigenfunctions, then a system is only stable if all its eigenvalues are positive. By varying two variables (e.g. inlet-enthalpy and power) a stability plane can be created, which is then used to interpret the results of parameter studies.

This thesis focuses on thermo-hydraulic instabilities and does not explore coupled neutronic instabilities. Not all thermo-hydraulicly unstable states are the same, there are numerous types of instabilities which can occur. The different types will be discussed in chapter 2. System instabilities in BWR's have been the subject of much research. Research projects into instabilities in supercritical fluids have mainly focussed on CO_2 as the temperatures and pressures needed to attain a supercritical state are much lower than for water.

There are a number of books on thermohydraulic instabilities. Lahey and Moody [14] focus on the thermohydraulics in nuclear power reactors and explains Ledinegg instabilities and includes a large frequency domain analysis

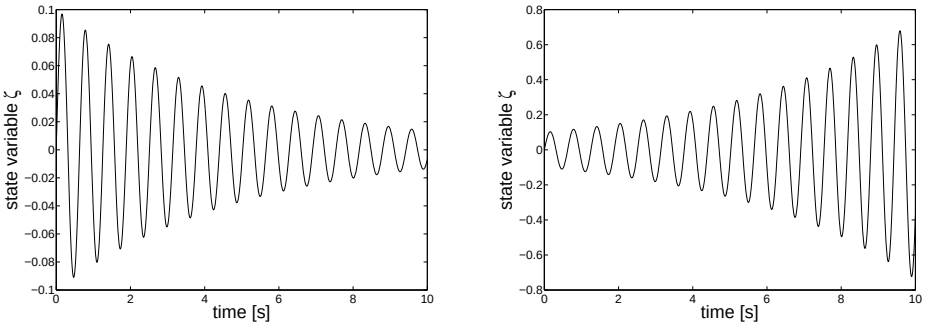

(a) Stable system (b) Unstable system

Figure 1.4: Perturbations in a stable system dampen, while perturbations in an unstable system grow.

of density wave oscillations (DWO) as well as coupling DWO, to neutronics. The book steam power engineering, edited by Ishigai [10], discussed a number of different flow instabilities from an engineering point of view.
A number of articles have been written on the subject of thermohydraulic instabilities in BWR's, the most of important of which are named below. Boure et al [2] suggest a way of classifying the different instabilities which have been observed. March-Leuba et al. [17] have published a state of the art review on coupled thermohydraulic-neutronic instabilities which focusses on density wave oscillations.

1.4 Previous Work

Though there has been much research into the stability of heated two phase flows such as in BWR's, the research into the stability of supercritical water loops and especially stability of the HPLWR is very limited. There have been no experimental (scaled) facilities to investigate supercritical water instabilities so far. There has been some numerical research into supercritical water instabilities. Natural circulation loops under supercritical conditions have been studied (numerically) by P.Jain et al.[11] and R.Jain et al.[13]. Both include comparisons to existing CO_2 natural circulation loops. CO_2 is however a poor scaling fluid since its dimensionless density does not match that of water. Ortega Gómez has numerically studied the stability characteristics of the HPLWR using COMSOL [19]. Ortega Gómez included a parameter study of a single channel core including hydraulic diameter, inlet and outlet constrictions, external pressure drop and length of the core. Chatoorgoon et al.[5] investigate non-dimensional parameters which affect the stability of supercritical water system. Cheng et al.[6] developed a model: the point-hydraulics model (PHM) and compare it to a code system: SASC.

1.5 Objectives

As in BWR's the HPLWR is expected to present instabilities, especially since the change in density is greater in a HPLWR than in a BWR. This thesis is part of a larger project investigating instabilities in the HPLWR design. The project involves a scaled Freon R23 facility (DeLight - Delft Light water reactor) [22], built at the Delft University of Technology. The project focusses on investigating the thermohydraulic instabilities which could be present in the single pass HPLWR concept as well as in the three pass HPLWR concept. The aim of this research project is twofold:

- Create a code which can investigate supercritical systems
- Investigate the applicability of the DeLight experimental facility with respect to HPLWR stability
- Investigate stability of HPLWR design choices

The scaled HPLWR facility DeLight

The experimental facility DeLight is a scaled version of the cooling loop in the HPLWR design [22]. Freon R-23 was chosen as the scaling fluid to be used. Furthermore a number of assumptions were made to arrive at the scaling laws used to design DeLight. To be able to correctly interpret the results obtained from DeLight the effect of using Freon and the effect of the assumptions made to create DeLight will be investigated in this thesis.

Parameter investigation of HPLWR design

For the single pass core a number of parameters have already been studied by Ortega Gómez [19]. Parameters such as the effect of inlet and outlet friction's as well as hydraulic diameter, length and pressure drop. This thesis will look into the effect on stability of:

1. System pressure
2. Power distribution in a three pass core
3. Friction caused by mixing planes in three pass core

1.6 Outline

In chapter 2 the main governing equations will be derived and the mechanics behind the instabilities will be explained. The scaling laws used to build the DeLight facility as well as the assumptions made to arrive at these scaling laws, are described towards the end of chapter 2. Finally a discussion about

the different possible dimensionless numbers can also be found in chapter 2. The numerics of the code and COMSOL will be explained in chapter 3 along with an investigation into the effect of the different definitions of the equation of state of the fluids. In chapter 4 the effect of using Freon-23 as the scaling fluid is investigated. This is followed by a closer look at the different assumptions made to arrive at the scaling laws used to develop DeLight. In chapter 5 the different HPLWR design choices will be investigated, including power distribution, three pass core setup and the effect of the friction due to mixing planes in the three pass core. The findings will be summarised in the chapter 6 which includes a discussion of the findings as well as the conclusions which may be drawn from these findings and recommendations on future research.

Chapter 2

Theory

2.1 Governing Equations

The thermo-hydraulics in the HPLWR is governed by the equations of conservation: mass, momentum and energy. Due to the complex behaviour of the density of water in a supercritical state a number of simplifications are made in the model used to simulate the HPLWR. The most important one is using a one dimensional model, which makes a stability analysis of the system feasible. Another crucial simplification is the way in which heat is transferred to the bulk of the fluid. Since the model is one dimensional and each cross-secitonal volume element has only one area averaged enthalpy, there can be no radial conduction or mixing within the cooling fluid itself. An important interaction which has not been modelled is the fission rate (power) to density (or 'void') feedback mechanism. Both the heat transfer and the power-void feedback are not included in this work, but should be added in further investigations.

The Equation of State

In general, the equation of state of a fluid is dependent on the enthalpy and pressure of the fluid. The water in the HPLWR is at $250bar$ ($\sim 25MPa$) while the pressure drop over the core is approximatly $150kPa$, two orders of magnitude less than the system pressure. As a simplification the dependence of the equation of state on the pressure of the system has therefore been neglected. The influence of doing so will be investigated in section 3.7 The data needed to create a model for the equation of state of water and Freon R-23[1] is extracted from the National Institute of Standards and Technology database [15]. The equation of state can be modelled in two ways; by using a polynomial expression or by using a spline. In the case of the polynomial the accuracy of the model can be increased by increasing the

[1] scaling fluid used in experimental setup see section 2.4.3

degree of the polynomial, while the spline (in this case a cubic spline) can be improved by increasing the number of points (knots) along which it is defined. The data points extracted from the NIST database are fitted using the Matlab curve fitting toolbox. The system (especially its stability) is very sensitive to the equation of state model used (see [13, 19]), so the influence of such a model on the stability is investigated in section 3.6. The properties of Freon-23 at $5.7MPa$ are shown in Fig. 2.1.
The

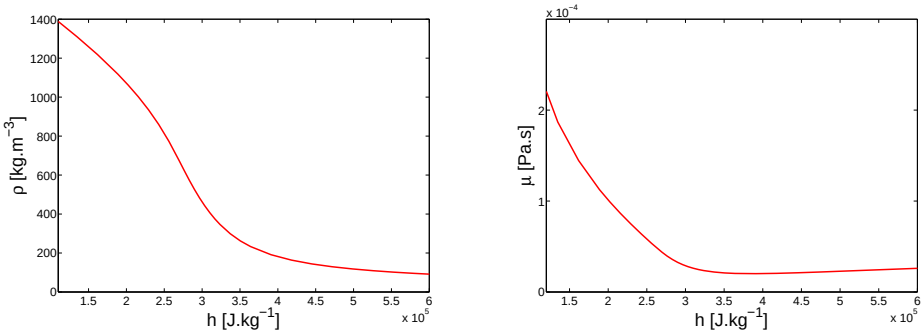

(a) Density of Freon-23 (b) Viscosity of Freon-23

Figure 2.1: Properties of Freon-23 as a function of enthalpy at the nominal pressure of 5.7MPa.

Conservation of Mass

The conservation of mass equation in its general form is stated below. All variables are averaged over the cross-section. For simplicity's sake the over-bars to denote the averages have been left out.

$$\frac{\partial \rho}{\partial t} + \frac{\partial \rho u}{\partial x} = 0, \tag{2.1}$$

where u is the velocity in the positive x direction and ρ is dependent on both space and time. Conservation of mass can be rewritten in terms of enthalpy, mass flux and specific volume:

$$\frac{\partial \rho}{\partial t} = \frac{\partial \rho}{\partial h}\frac{\partial h}{\partial t} = \frac{\partial 1/v}{\partial h}\frac{\partial h}{\partial t}, \tag{2.2}$$

giving:

$$
\begin{aligned}
-\frac{1}{v^2}\left(\frac{\partial v}{\partial h}\right)\frac{\partial h}{\partial t} &= \frac{\partial G}{\partial x} \\
\frac{\partial h}{\partial t} &= v^2\frac{\partial G}{\partial x}\left(\frac{\partial v}{\partial h}\right)^{-1},
\end{aligned} \tag{2.3}
$$

where G is the mass flux ($= \rho u$), v the specific volume ($= \rho^{-1}$) and h is the enthalpy.

Conservation of Momentum

The general form of the conservation of momentum equation is taken as the starting point of the derivation.

$$
\frac{\partial \rho\vec{v}}{\partial t} + \nabla\cdot\vec{v}\rho\vec{v} = -\rho\vec{g} - \nabla p + \nabla\cdot\vec{\vec{T}} \tag{2.4}
$$

The following assumptions have been made implicitly: the only external body force is gravity, the fluid simulated is isotropic i.e. the stress tensor $\vec{\vec{\sigma}}$ is symmetric so it can be separated into a pressure component and the deviatric stress tensor $\vec{\vec{T}}$. Using cylindrical symmetry, taking cross-sectional averages, and assuming super-critical water behaves like a Newtonian fluid[2] the momentum conservation equation becomes:

$$
\frac{\partial \overline{\rho}\,\overline{u}}{\partial t} + \frac{\partial \overline{\rho}\,\overline{u}^2}{\partial x} + \frac{\partial \overline{(\rho u'^2)}}{\partial x} = -\overline{\rho}g - \frac{\partial \overline{p}}{\partial x} + \frac{\partial \sigma_{xx}}{\partial x}, \tag{2.5}
$$

where $\sigma_{xx} = \mu\left\{2\frac{\partial \overline{u}}{\partial x} - \frac{2}{3}\nabla\cdot\vec{v}\right\}$ and the variation of u from the average $\overline{u}$ is denoted by u'.Two of the above terms represent the friction loss and can be grouped together and parametrised:

$$
-\frac{\partial \overline{(\rho u'^2)}}{\partial x} + \frac{\partial \sigma_{xx}}{\partial x} = \frac{\overline{G}^2}{2\rho}\left\{\frac{f}{D_H} + \sum_i K_i\right\}, \tag{2.6}
$$

where f is the friction factor which is approximated using the Darcy-Weisbach relation in its explicit form as developed by Haaland [9].

$$
f = \left[-1.8log\left(\left(\frac{\epsilon}{3.7D_H}\right)^{1.11} + \frac{6.9}{Re}\right)\right]^{-2} \tag{2.7}
$$

A second option is the McAdams and Blasius relation which is used by Prashant Jain [11]:

[2]Assuming supercritical water acting as a newtonian fluid allows us to describe it in terms of dynamic viscosity μ

$$f = \begin{cases} 0.316Re^{-0.25} & Re < 30000 \\ 0.184Re^{-0.20} & 30000 < Re < 10^6 \end{cases} . \tag{2.8}$$

The Darcy-Weisbach form, however, will be used throughout our simulations. The conservation of momentum equation becomes:

$$\frac{\partial G}{\partial t} + \frac{\partial G^2 v}{\partial x} = -\frac{g}{v} - \frac{\partial p}{\partial x} - \frac{G^2 v}{2}\left\{\frac{f}{D_H} + \sum_i K_i \delta(x - x_i)\right\}, \tag{2.9}$$

where all overbars have been left out for clarity.

Conservation of Energy

The last conservation equation is that of energy:

$$\frac{\partial \rho e}{\partial t} + \nabla \cdot \rho e \vec{v} = \frac{\partial p}{\partial t} + \vec{v} \cdot \nabla p + \nabla \cdot \lambda \nabla T + \mu \Phi, \tag{2.10}$$

where e is the energy per unit mass, λ is the heat conduction coefficient and Φ is the heat generated by friction. The energy e is composed of kinetic, potential and internal energy. The potential and kinetic component of the energy term have been neglected as they are small relative to the internal energy of the cooling fluid. Furthermore equation (2.10) can be simplified using the equation of mass (2.1)

$$\begin{aligned} \frac{\partial \rho h}{\partial t} + \nabla \cdot \rho h \vec{v} &= \rho \frac{\partial h}{\partial t} + h \frac{\partial \rho}{\partial t} + \rho \vec{v} \nabla h + h \nabla \cdot \rho \vec{v} \\ &= \rho \left(\frac{\partial h}{\partial t} + \vec{v} \nabla h \right) + h \left(\frac{\partial \rho}{\partial t} + \nabla \cdot \rho \vec{v} \right) \\ &= \rho \left(\frac{\partial h}{\partial t} + \vec{v} \nabla h \right) \end{aligned} \tag{2.11}$$

Subsequently pressure effects, axial heat conduction and friction are neglected, and cross-sectional averages are taken:

$$\overline{\rho \frac{\partial h}{\partial t}} + \overline{\rho u \frac{\partial h}{\partial x}} = \overline{\frac{\partial}{\partial y} \lambda \frac{\partial T}{\partial y}} + \overline{\frac{\partial}{\partial z} \lambda \frac{\partial T}{\partial z}} = \frac{q'' P_H}{A}, \tag{2.12}$$

which leads us to:

$$\frac{\partial h}{\partial t} + Gv \frac{\partial h}{\partial x} = \frac{q'' P_H v}{A} \tag{2.13}$$

2.2 Pressure Nomenclature

Due to the confusion which may arise, this section explains from the pressure terminology as used in Ortega Gómez et al.([18, 19]) in detail and emphasises the differences between the definitions used throughout the code.

System Pressure

The pressure at which the system is operating is called the system pressure, which is 25 MPa in the case of the HPLWR. The system pressure mainly determines the equation of state. When referring to the system pressure it will be clearly stated as such.

Pressure

The pressure varies throughout the system due to gravity, friction, acceleration and, if applicable, an external source (e.g. a pump). These pressure variations over the core are of the order of 150kPa, which is less than one percent of the system pressure. This pressure variation is denoted with p, without any sub- or superscripts and referred to as the pressure.

Pressure Drop

The pressure drop is defined as the difference between the inlet and outlet pressure (including the pressure drop over the entrance K_{in} and exit orifices K_{out}) and denoted by p_{drop} (see Fig. 2.2), which is equal to the driving pressure of the pump. In the case of natural circulation, the driving pressure drop is caused by a buoyancy difference between the fluid in the core-riser section and the fluid in the downcomer.

Dynamic Pressure

The dynamic pressure, denoted by π is the sum of the local or 'static' pressure and the dynamic head $G^2 v$:

$$\pi = p + G^2 v \tag{2.14}$$

The pressure used in the numerical code is the dynamic pressure. This is done to improve convergence [18]. This has implications for the way the boundary conditions are implemented. The pressure at the inlet and outlet are as follows (see Fig. 2.2):

$$p_{in} = p_0 \tag{2.15}$$

$$p_{out} = p_0 + p_{drop} \tag{2.16}$$

Note that p_{drop} is a negative number. These boundary conditions must then be transformed into boundary conditions for the dynamic pressure π:

$$\pi_{in} = p_0 + G_{in}^2 v_{in} \tag{2.17}$$
$$\pi_{out} = p_0 + p_{drop} + G_{out}^2 v_{out} \tag{2.18}$$

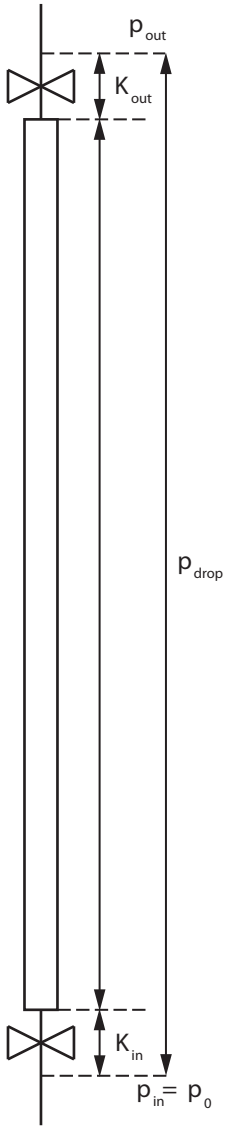

Figure 2.2: View of a single channel with the in and outlet pressures defined. p_0 is in this case the system pressure. The K values are the in- and outlet friction coefficients

Note that even though the convective term $G^2 v$ is added to the pressure

to obtain the dynamic pressure, what is actually being done is eliminating the dependence of π on the convective term,

$$\begin{aligned} \frac{\partial p}{\partial x} &= -\frac{\partial G^2 v}{\partial x} - \frac{g}{v} + \frac{G^2 v}{2}\left(\frac{f}{D_H} + \sum_i K_i\right) \\ \frac{\partial G^2 v + p}{\partial x} = \frac{\partial \pi}{\partial x} &= -\frac{g}{v} + \frac{G^2 v}{2}\left(\frac{f}{D_H} + \sum_i K_i\right), \end{aligned} \tag{2.19}$$

which is only dependent on the gravitation and friction due to the wall and in- and outlet orifices.

2.3 Instabilities and their classification

The HPLWR does not always lead to a stable system, hence instabilities can occur. These instabilities have been extensively studied in the BWR setting [3, 14, 16]. The instabilities can be divided into two categories: static and dynamic [2]. In contrast to what its name suggests, static instabilities do vary in time. A static instability can be analysed using the steady state equations only. There are two types of static instabilities which are considered here:

- Flow excursions or Ledinegg instabilities
- Flow maldistribution

Ledinegg Instability

A Ledinegg instability, also known as Flow Excursion, is best explained using Fig. 2.3. Given a certain flow rate m, a channel will cause a pressure drop Δp due to friction losses and gravity (dashed lines in Fig. 2.3) which depends on the fluid/vapor mixture flowing through the channel. For single phase flows (i.e. vapour or liquid) a higher mass flux results in a higher pressure drop as exhibited by the lines labeled "all vapor" and "all liquid". In a heated channel, however, a smaller mass flux creates a larger enthalpy or temperature jump which causes the cooling fluid to change its composition. This change in composition can cause a lower mass flux to result in a higher pressure drop and, more importantly, a certain pressure drop (i.e. the imposed external pressure drop, marked Δp_{pump}) will correspond to multiple steady state situations with various possible mass fluxes. Some of these steady states will be stable and some will be unstable. For example the point labeled 0 in Fig. 2.3, is an unstable state, the two other intercepts are stable states. A small perturbation of a stable steady state will be dampend. If, however, a large enough perturbation occurs, the system jumps to

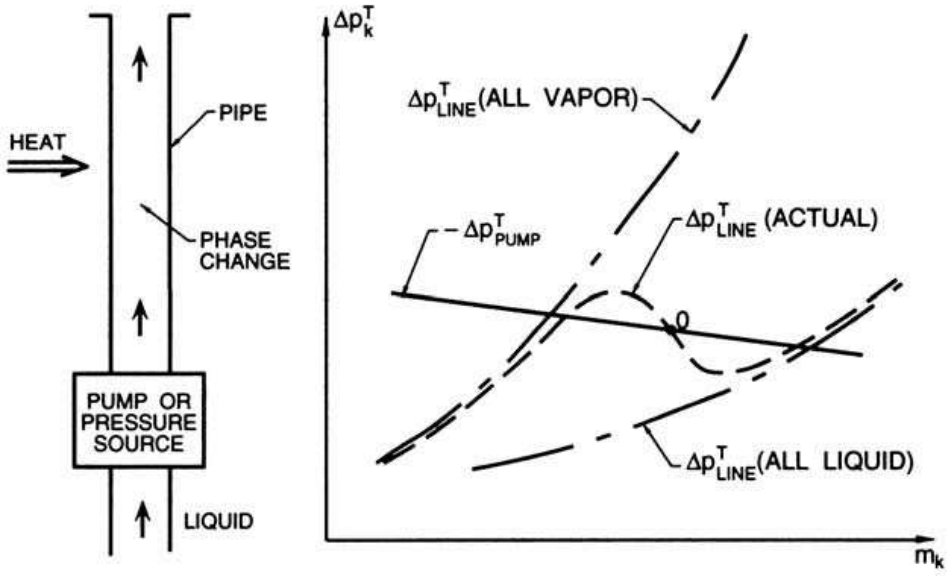

Figure 2.3: Pressure drop vs mass flux. When the pressure due to the pump, is larger than the pressure drop due to friction in the channel the flow increases and visa versa [4]

the other steady state with a different characteristic flow. This phenomenon is called a flow excursion or Ledinegg instability. To avoid Ledinegg instabilities one can alter the characteristics of the pump so as to avoid multiple stable points. In general the steeper the gradient of the pump in the Δp, m (mass flow rate) plane the less chance of the Ledinegg instabilities.

Flow Maldistribution

A flow maldistribution takes place in a case where multiple heated channels are given a common fixed mass flux ($G_1 + G_2 = G_{total}$). When one of the channels experiences a flow excursion the other channels have to accommodate to this. This phenomenon is extremely difficult to predict if a large number of channels is involved such as in a reactor core. To avoid this type of instability, channels are given a large negative resistance characteristic [3]. This is kind of instability is unique to parallel channel systems, and thus will not appear in this work.

Density Wave Oscillations

Density wave oscillations (DWO) are dynamic instabilities and cannot be predicted using the steady state equations. DWO's have been extensively

[3] A larger flow rate causing a smaller pressure drop

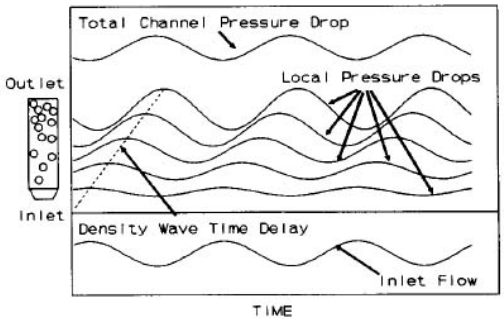

Figure 2.4: Illustration of the local pressure drop delay introduced by the density wave oscillation mechanism. [17]

studied in BWR's [3, 10, 16, 17, 20] and it is known that the onset of DWO is strongly dependent on the height of the boiling boundary. Another important factor in determining the onset of DWO's is the ratio of the in-phase pressure drop (pressure loss in the high density region) to the out of phase pressure drop (pressure loss in the low density region) [18]. In a supercritical fluid the equivalent of the boiling boundary is the pseudo-critical point. The DWO is driven by two concepts, the magnification of the amplitude of pressure drop fluctuations and the time taken by the perturbation to traverse the core.
A flow perturbation in the core section will cause an enthalpy wave, which takes a finite time to traverse the core. The enthalpy wave will be accompanied by a corresponding local pressure drop wave[4]. The amplitude of this pressure drop wave increases as it moves through the core, due to the expansion of the cooling fluid. The sum of all the local pressure drops determines the total pressure drop over the core. The time taken to pass through the core can cause the pressure wave to be out of phase with the initial flow perturbation. In Fig. 2.4 an example is shown of a 180 degree phase shift. The 180 degree phase shift causes the lowest pressure drop over the core to coincide with an already larger mass flow. Since the pressure drop over the core at that moment is smaller than the externally imposed pressure drop (e.g. a pump or large bypass) the mass flux will increase thus further increasing the flow rate and amplifying the perturbation.

2.4 Scaling the System

Investigating the physics and instabilities of the HPLWR would be expensive if done using an experimental supercritical water facility. This would require a large experimental setup up to able to withstand pressures exceed-

[4] An increase in enthalpy causes a decrease in density which causes larger local velocities to maintain the mass flux. The increase in local velocity in turn leads to an increased wall-friction and pressure drop.

ing $25MPa$ and wall temperatures of upto 620°C[23]. A choice was made to use Freon-23 as a substitute for water [22] because its dimensionless density matches that of water at a certain pressure. The scaling rules, based on Freon-23, were developed by Rohde et al.[22], allowing for a 600°C reduction in temperature and a $20MPa$ reduction in pressure. The dimensionless equations and the resulting scaling rules will be derived again below, starting from the governing equations derived in the section 2.1.

2.4.1 Dimensionless Equations and Numbers

Making the conservation of mass equation dimensionless is a straightforward task, however, a careful choice of constants is needed to make the dimensionless equation relevant and useful. The variables have been non-dimensionalized in the following way:

$$x^\star = \frac{x}{L_c}, h^\star = \frac{h}{h_{pc}}, v^\star = \frac{v}{v_{pc}}$$
$$t^\star = \frac{t}{\frac{L_c}{G_c v_{pc}}}, G^\star = \frac{G}{G_c}, p^\star = \frac{p}{G_c^2 v_{pc}}$$

Most non-dimensionalizing parameters are very intuitive. This leads to the following dimensionless equations:
conservation of mass,

$$\frac{\partial h^\star}{\partial t^\star} = v^{\star^2} \frac{\partial G^\star}{\partial x^\star} \left(\frac{\partial v^\star}{\partial h^\star} \right)^{-1}, \tag{2.20}$$

conservation of momentum,

$$\frac{\partial G^\star}{\partial t^\star} + \frac{\partial G^{\star^2} v}{\partial x^\star} = -\frac{1}{N_{Fr} v^\star} - \frac{\partial p^\star}{\partial x^\star} - \frac{G^{\star^2} v^\star}{2} \left\{ \frac{f}{D_H^\star} + \sum_i K_i^\star \right\}, \tag{2.21}$$

where N_{Fr} is the froude number and the friction factor f is dependent on the Reynolds number and the relative roughness: $f(Re, \frac{\epsilon}{D_H})$. The Froude number is given by:

$$N_{Fr} = \frac{G_c^2 v_{pc}^2}{L_c g} \tag{2.22}$$

Conservation of energy

$$\frac{\partial h^\star}{\partial t^\star} + u^\star \frac{\partial h^\star}{\partial x^\star} \quad = \quad v^\star N_{\Delta h}, \tag{2.23}$$

where $N_{\Delta h}$ is the dimensionless enthalpy jump which resembles the phase-change number used in two-phase flow systems. This number is mentioned as $N_{Pseudo-Phasechange}$ in Rohde et al. [22].

$$N_{\Delta h} = \frac{q'' P_H}{A} \frac{L_c}{h_{pc} G_c} = q_w \frac{L_c}{h_{pc} G_c} = \frac{P}{h_{pc} G_c A} \tag{2.24}$$

Note the difference between the three power quantities: q'', q_w and P. P is the total power applied to the channel, q_w is the power per unit volume of core (q_w is used in COMSOL) and q" is the heat flux (power per unit area of channel/cladding surface).

2.4.2 Stability Plane and Dimensionless Numbers

In section 2.4 three dimensionless numbers were created, the Froude number, friction number and a third dimensionless number, which resembles the phase-change number or Zuber number as used in two phase systems [21].

$$N_{\Delta h} = \frac{q'' P_H L_c}{h_{pc} A_{x-s} G} \tag{2.25}$$

This dimensionless number is an indicator of the enthalpy change experienced by the cooling liquid during its passage through the core. The number will be referred to as the dimensionless enthalpy jump $N_{\Delta h}$ and contains two operational parameters, i.e. the power and the flow:

$$N_{\Delta h} = \frac{h(L_c) - h_{in}}{h_{pc}} = \frac{q'' P_H L_c}{h_{pc} A_{x-s} G} \tag{2.26}$$

To fully define the operational point of the system in steady state there is need for one more dimensionless number, which is the sub-cooling number defined as:

$$N_{sub} = \frac{h_{pc} - h_{in}}{h_{pc}} \tag{2.27}$$

The sub-cooling number is the dimensionless form of the inlet enthalpy which, together with the geometry and pressure of the system and the dimensionless enthalpy jump, completely define any steady state. Thus, given a certain geometry the enthalpy jump vs sub-cooling plane spans all possible operational points. This plane allows us to compare the HPLWR and the scaled facility, DeLight.
The sub-cooling number was given and explained heuristically above. It can be derived from the steady state energy conservation equation as can be

seen in the derivation below:

$$\begin{aligned} G\frac{\partial h}{\partial x} &= \frac{q'' P_H}{A_{x-s}} \\ \int_0^{\lambda} \frac{\partial h}{\partial x}.dx) &= \int_0^{\lambda} \frac{q'' P_H}{A_{x-s} G}.dx \\ h_{pc} - h(0) &= \frac{q'' P_H L_c}{A_{x-s} G} \frac{\lambda}{L_c} \\ N_{sub} &= N_{\Delta h} \frac{\lambda}{L_c} \end{aligned} \tag{2.28}$$

where λ is the height at which the cooling fluid reaches the pseudo-critical enthalpy. This derivation gives us an interesting insight into the relationship between the dimensionless enthalpy jump and the sub-cooling number. It seems that the sub-cooling number is dependent on the enthalpy jump which would make the two numbers less suitable to describe the system since this would prevent varying the dimensionless numbers independently. The subcooling number, however, is dependent on the inlet enthalpy and $N_{\Delta h}$ is not, hence the dimensionless numbers are independent of each other. λ is a function of both N_{SUB} and $N_{\Delta h}$. Varying one of these dimensionless numbers also changes λ but does not affect the other

Alternative Dimensionless Numbers

The governing equations can also be made dimensionless by creating a time constant, the frequency of fluid expansion used by Ortega Gómez [18], which is defined as follows:

$$\begin{aligned} \Omega_p &= \left(\frac{\partial v}{\partial h}\right)_p G\frac{dh}{dz} = \left(\frac{\partial v}{\partial h}\right)\frac{q'' P_H}{A_{x-s}} \\ \overline{\Omega_p} &= \frac{1}{L_c}\int_0^{Lc} \Omega_p dz = \frac{G}{L_c}\Big(v(L_c) - v(0)\Big) \end{aligned} \tag{2.29}$$

This leads to dimensionless numbers called the pseudo-phase change and the pseudo-subcooling numbers:

$$N_{P-PCH} = \frac{\overline{\Omega_p} L_c}{u(0)} = \frac{v(L_c) - v(0)}{v(0)} = \frac{u(L_c) - u(0)}{u(0)} \tag{2.30}$$

$$N_{P-sub} = \frac{v(L_c) - v(0)}{v(0)} \frac{\overline{\Omega_p}\lambda}{u(0)} = N_{P-PCH}\frac{\lambda}{L_c} \tag{2.31}$$

The relation between the dimensionless numbers defined in equations (2.30) and (2.31) is the same as the relation of those defined in equations (2.25) and

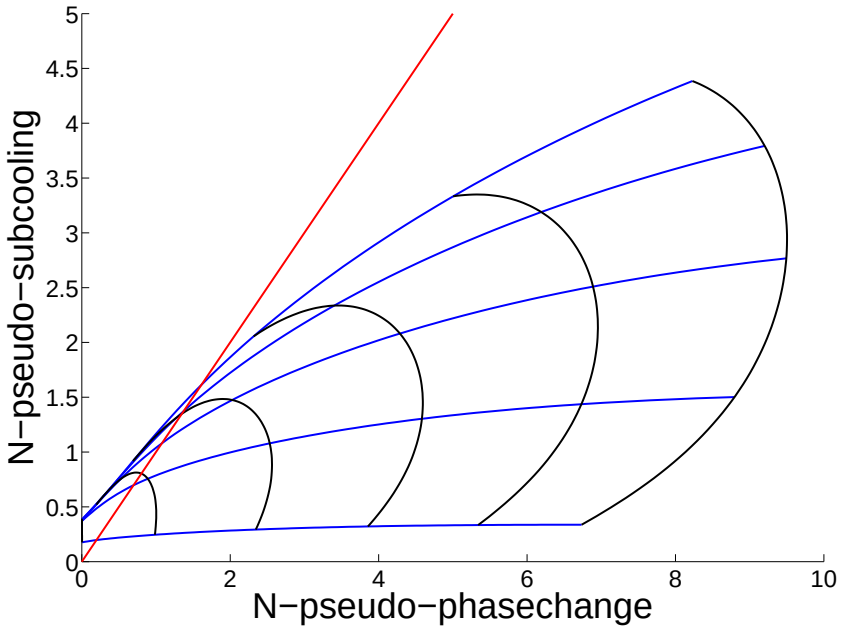

Figure 2.5: Iso-exit-enthalpy (blue) and iso-power (black) lines in the pseudo-subcooling and pseudo-phasechange plane. The red line represents a special iso-exit enthalpy line: $h_{out} = h_{pc}$

(2.27). The definitions of the dimensionless numbers used by Ortega Gómez et al [19], however, do depend on each other. In other words, a change in the inlet enthalpy not only changes the pseudo-sub-cooling number but also affects the pseudo-phase change number. In a similar manner a change in power affects both the pseudo-phase change number and the pseudo-sub-cooling number. The implications of the definitions of Ortega Gómez can be made clearer by mapping the first set dimensionless numbers on the second set of dimensionless numbers:

$$\begin{aligned} N_{P-PCH} &= \frac{v(N_{\Delta h} h_{pc} + h_{in}) - v(h_{in})}{v(h_{in})} \\ &= \frac{v\Big(h_{pc}[N_{\Delta h} + 1 - N_{sub}]\Big) - v\Big(h_{pc}[1 - N_{sub}]\Big)}{v\Big(h_{pc}[1 - N_{sub}]\Big)} \end{aligned} \tag{2.32}$$

In Fig. 2.5, the graphical version of the mapping can be seen. The red line is the locus of all operational points where the pseudo-critical enthalpy at the exit of the core is reached. The distortion of the stability plane makes it more difficult to interpret stability plots and can suggest physical phenomena which are not actually present as can be seen in Fig. 2.6. Fig. 2.6a uses the

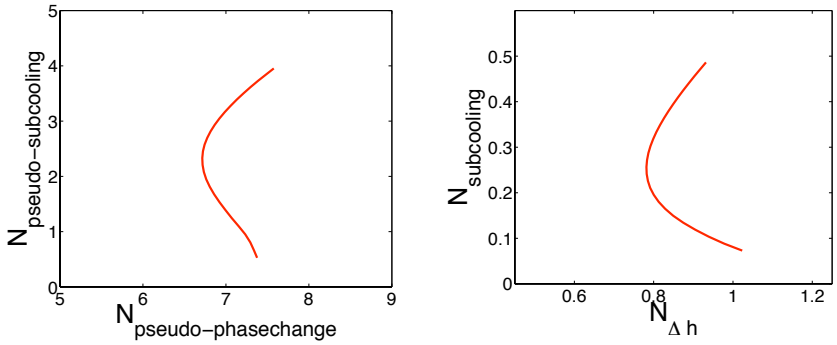

(a) Dimesionless number as used by Ortega Gomez [19]

(b) Dimensionless numbers as developed by Rohde et al. [22]

Figure 2.6: A neutral stability line in two stability planes

alternative dimensionless numbers and in its lower sub-cooling region the increased negative gradient seems to suggest that there is a destabilizing mechanism in the system for low subcooling numbers. This, however, is purely a result of the definition of the alternative dimensionless numbers.

Both sets of dimensionless numbers show similarities with the Ishii-Zuber stability map which is traditionally used in BWR analysis. This means that lines which are parallel to the line $N_{(P-)SUB} = N_{(P-)PCH}$ are iso-exit enthalpy lines. The iso-exit enthalpy line which goes through the origin represents all operational points that reach the pseudo-critical point exactly at the exit of the core. Straight lines through the origin represent all steady states which reach a certain reference enthalpy at the same height.

2.4.3 Three Scaled Systems

Making the governing equations dimensionless produces three dimensionless numbers, $\frac{f}{2D_H}$, N_{Fr} and $N_{\Delta h}$, which must be kept the same to preserve the physics present in the system [22]. Rohde et al derive the scaling laws as follows:

$$\begin{aligned} N_{Fr}^{R-23} &= N_{Fr}^{H_2O} \\ \left.\frac{G_c^2 v_{pc}^2}{L_c g}\right|_{R-23} &= \left.\frac{G_c^2 v_{pc}^2}{L_c g}\right|_{H_2O} \\ \frac{L_c^{R-23}}{L_c^{H_2O}} = X_L &= X_G^2 X_v^2 \end{aligned} \tag{2.33}$$

The scaling law in equation (2.33) describes the scaling of the length dimension and is derived from keeping the Froude number constant. The scaling for the power can be derived from keeping the dimensionless enthalpy jump,

$N_{\Delta h}$, the same for both systems.

$$X_P = X_h X_G X_A = X_h X_G X_L^2 = X_h X_G^5 X_v^4 \tag{2.34}$$

or

$$X_{q_w} = \frac{X_h X_G}{X_L} = \frac{X_h}{X_G X_v^2} \tag{2.35}$$

One more scaling law is required to uniquely define a scaled system. For this friction factor needs to be kept constant. The friction factor, however, is dependent on the Reynolds number and the relative roughness ($\frac{\epsilon}{D_H}$). Ideally, the Reynolds number and the relative roughness should be kept the same (these are in themselves dimensionless numbers). Thus ensuring that the friction factor remains exactly the same.
Freon 23 was selected due to its scaling potential and its close match in density as a function of enthalpy. The viscosity of Freon 23, however, does not match so well, making it difficult to keep the Reynolds number constant and a choice needs to made which leads to two distinct scaling systems and an experimental facility which has been built at the TU Delft
Below three systems are presented and discussed. The first system attempts to preserve all the physics present in the HPLWR, the second is a scaled version of the HPLWR which can be cooled by natural circulations and the third is the experimental setup at the Delft University of Technology.

The HPLWR Scaled

The last dimensionless number which needs to be kept constant is the friction factor. The friction factor is in itself a function of two dimensionless quantities: the relative roughness $\frac{\epsilon}{D_H}$ and the Reynolds number, eq. (2.7). If it were possible to keep the Reynolds number and relative roughness constant this would lead to the scaling rules derived in eq. (2.36) and summed up in table 2.1.

$$N_{Re} = \frac{GD_H}{\mu}\bigg|_{H_2O} = \frac{GD_H}{\mu}\bigg|_{ideal}$$
$$X_G = X_\mu X_L^{-1} \tag{2.36}$$

This set of rules leads to a system which would accurately replicate the physics within the HPLWR [5]. The friction present in this system would, however, prevent the system from being cooled by solely by natural circulation. Additionally it is difficult to make the roughness of the channel to specification and keep the Reynolds number constant. Thus to be able to experiment on an HPLWR cooled by natural circulation this system would not suffice. This leads us to the next system which will be discussed, which

[5] assuming that the equations used to model the HPLWR are correct

X_G	1.308
X_L	0.627
X_{q_w}	0.281
X_P	0,068

Table 2.1: Scaling laws of for scaling the HPLWR for Freon

is a scaled version of the HPLWR which can also operate under natural circulation conditions. This system will also serve as a useful research tool in chapter 4.

A Scaled Natural Circulation HPLWR

To be able to operate the system under natural circulation conditions the friction in the system needs to be reduced. Rohde et al.[22] suggest, that the Darcy-Weisbach friction factor does not necessarily need to be kept constant to preserve the stability behaviour of the system but as long as the relative distribution of friction along the heated channel remains the same, the stability will not be affected. This means it is possible to reduce the friction allowing for cooling by natural circulation. Instead of attempting to equate the Reynolds numbers (and thus the friction factors) an attempt is made to create the same friction profile. Thus by trial and error the friction factor was scaled in such a way that its profile closely resembled that of the HPLWR. It is important to remember that it is the friction factor's profile and not its absolute value which is of importance to the stability of the system. This completes the set of equations and gives a unique set of scaling rules, determined by the water to Freon ratios: X_v, X_h and X_μ, which are listed in table 2.2. These in turn lead to the rules developed by Rohde et al.[22] and listed in table 2.3. Note that the hydraulic diameter is not scaled using the same scaling rules as the length of the core.

X_v	0.605
X_μ	0.820
X_h	0.135

Table 2.2: Ratio of the density, viscosity and enthalpy of water to Freon at their respective pseudo-critical points

Experimental Setup, DeLight

The scaling rules developed in section 2.4.3 act as a blue print for the experimental facility named DeLight (DElft LIGHT water reactor). Some of the

X_G	0.740
X_L	0.201
X_{q_w}	0.498
X_P	0.079
X_{D_H}	1.114

Table 2.3: List of scaling laws for a natural circulation cooled HPLWR, [22]

dimensions could not be built exactly to specification (e.g. the hydraulic diameter should ideally be $5.98mm$), thus leading to a third system: DeLight. DeLight is only slightly different from the system in the previous section: The experimental setup being built at the TU Delft has an $80cm$ (differs by $0.2cm$) long core which is heated by a large electrical current ($200A$), thereby achieving a uniform heatflux over the entire stainless steel channel. The channels in the core have an internal diameter of $6mm$, which differs by $0.02mm$ from the ideal dimension for the scaled facility. The facility is designed to operate as either a three parallel channel single pass core or a single channel three pass core, as can be seen in Fig. 2.7. The facility is optimized to reduce friction to allow for experiments involving natural circulation cooling. Each core tube is equiped with 10 thermocouples to accurately measure the temperature of Freon-23. Pressure drop measuring devices are installed at local constrictions to measure the friction caused by the constrictions. The flow rate is measured at the core inlet and induced by the pump installed into the downcomer. The downcomer and riser have a larger hydraulic diameter replicating the larger diameters present in the HPLWR. In Fig. 2.7 between bend 16 and 19 the facility can be set to bypass the pump thus cooling itself using only natural circulation. Furthermore the system is kept at the appropriate pressure by a pressure controller above the riser and before the downcomer. The downcomer is split and partly heated to simulate the effect of passing the cooling fluid through the moderator rods as is being planned in the most recent design of the HPLWR.

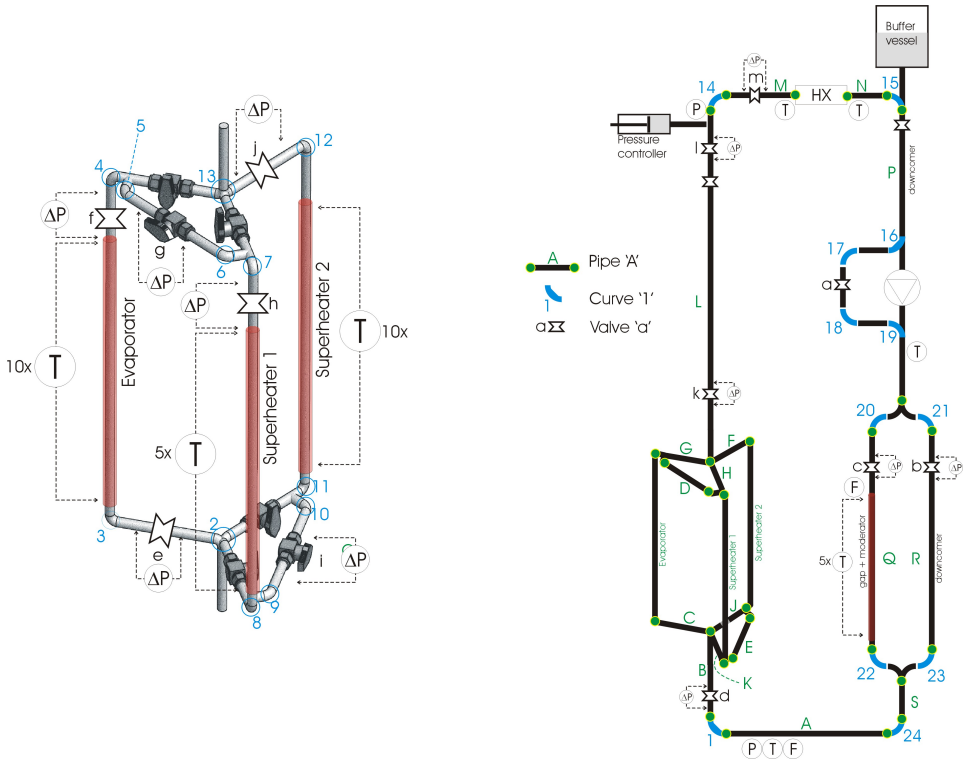

Figure 2.7: Experimental setup (DeLight) being built at Delft University of Technology. On the left side a detail of the core section describing the location of temperature (T), pressure drop (ΔP), absolute pressure (P) and flow (F) sensors

Chapter 3

Numerics

There are two ways to investigate instabilities: numerical simulations and experimental facilities. Since the experimental facility was not yet completed at the time of this thesis, the thesis will be solely concerned with numerical investigations. Ortega Gómez had already developed a numerical code which could simulate the core of the HPLWR and was written in COMSOL. This code was provided to the TU Delft and was used as base from which to develope a steady state code able to simulate multiple systems (DeLight, single and three pass HPLWR), with different cooling fluids such as water, scaled water (see section 4.2) and Freon-23. Furthermore a code was developed which uses the results form the steady state code to find the neutral stability boundary (NSB) in the stability plane (N_{sub} vs. $N_{\Delta h}$). This chapter will start with a discription of COMSOL Multiphysics in general followed by a description of the steady state and stability codes which have been developed, validated and benchmarked. The final parts of the chapter will look into the sensitivity of the NSB code to: the mesh coarseness, implementation of the equation of state (EOS) and system pressure.

3.1 COMSOL

As mentioned above the steady state and stability codes were written using COMSOL Multiphysics. COMSOL is a commercial finite element method simulation environment, which groups a number of known solver algorithms such as GMRES and UMFPACK and includes a GUI. The main advantage of such a program is that one only needs chose the physics to be simuated and draw the geometry. The program allows for steady-state, time-dependent and eigenvalue calculations to be done without having to implement the governing equations separately for each different ßcalculation.
The program, however, is built to calculate standard situations with, for example incompressible fluids, or involving structural mechanics. Due to the commercial character of the engine the actual implementation of the

different algorithms cannot be checked. This is especially problematic when the code has problems converging. Furthermore the program does not lend itself to post processing of the results so it is advisable to write a command line script using the Matlab-COMSOL interface so that results can be used in a versatile way.

3.2 The Code

The code which was written during the course of this thesis is a combination of two main programs which together result in a stability plane. The steady state code requires a number of parameters which must be set manually (e.g. the hydraulic diameter and initial values). Once these are set and the steady state solver is started a number of choices can be made regarding the system which is to be used (HPLWR, DeLight, etc.) and the fluid (Freon and water) to be simulated. The program then solves the steady state problem and produces a `.mat` file named after the fluid, which has been simulated. This `.mat` file is required as input into the second program, the NSB calculation code. This program searches for the NSB between for a set of subcooling numbers. A schematic representation of the two programs is shown in Fig. 3.1 The two programs will be discussed in more detail bellow. Both code's can be found in full in the appendix D and E.

3.2.1 Steady State Code

The steady state code is based on a code written by Ortega Gómez [18]. Though much of the original code which was supplied has been changed, the implementation of the weak form to solve the equations, the choice of finite element structure and 4^{th} and 5^{th} order Lagrange elements are the work of Ortega Gómez. Ortega Gómex also highlighted that the mass conservation equation must be placed last [18].
The steady state solver requires a number of parameters which need to be set manual. These include: length of the core, hydraulic diameter, gravitational acceleration, in- and outlet constrictions, pressure drop over the core, channel roughness and power. Once these are set the steady state equations are solved for a simplified geometry using a coarse mesh. This solution is stored and will be used as an initial guess for the final solution. The in- and outlet constriction are then added to the geometry and the mesh is refined. The steady state equation are then solved for a second time using the first solution as an initial guess (see Fig. 3.1). The steady state solver produces a `.mat` file which contains all the information about the solution to the system as well as the system itself.

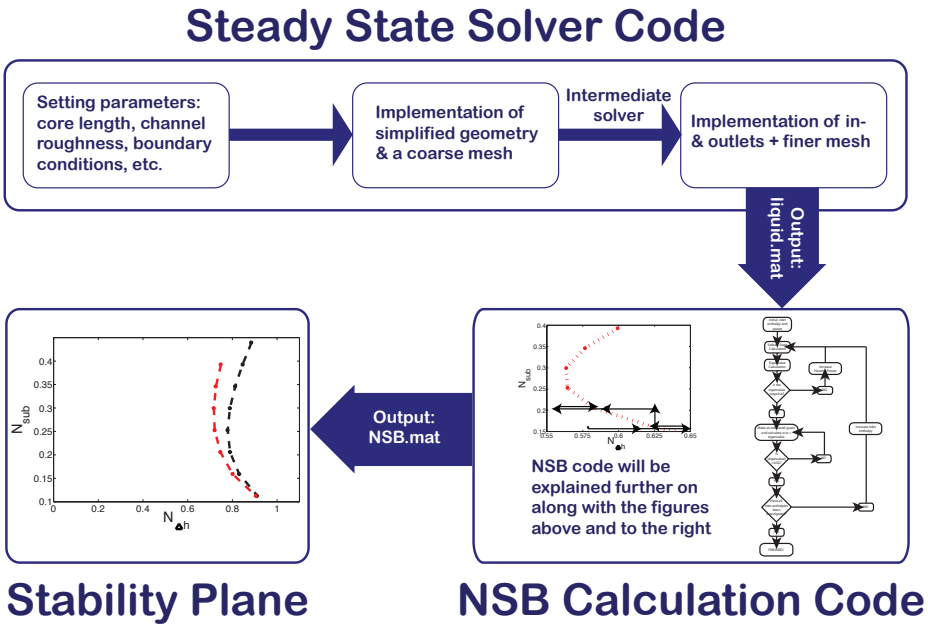

Figure 3.1: Schematic representation of the code used to develop a stability plane with a NSB. The steady state solver initializes all the required parameters for the NSB calculation code.

Boundary Conditions

The boundary conditions of the steady state solver proved to cause a problem, previous results could not be replicated using the boundary conditions in the program which was initially provided. The program which was provided to the TU Delft implemented the in- and oulet frictions as part of the boundary conditions in the following way:

$$h(0) = h_{in} \tag{3.1}$$

$$\pi(0) = (1 + \frac{K_{in}}{2})G(0)^2 v_{in} \tag{3.2}$$

$$\pi(L_H) = p_{drop} + (1 + \frac{K_{out}}{2})G(L_H)^2 v(L_H), \tag{3.3}$$

where h(0), G(0) and $\pi(0)$ are the enthalpy, mass flux and pressure at the inlet and $P(L_H)$ and $G(L_h)$ are the pressure and mass flux at $z = L_H$. All variables with a subscript are fixed (boundary) parameters of the system where p_{drop} is the external pressure drop to which the mass flux G must adjust itself.
This implementation by Ortega Gómez et al.[19] of the inlet and outlet

friction is confusing to reason with because the in- and outlet constrictions have an effect on the total pressure drop over the core, thus a simulation with constrictions cannot easily be compared to one without constrictions. Furthermore we were not able to replicate the results published by Ortega Gómez et al. [19] using the method described. Thus an alternative to this method was devised. By adding a small unheated length of channel to both ends of the core (see Fig. 3.2), the results of Ortega Gómez et al. were reproduced. The friction can be modelled in such a way that the effect of the extra piece of channel is exactly the same as the pressure loss coefficient of the orifice, see eq. (3.4). Though the method is numerically slightly heavier the results are easier to interpret and match previous results.

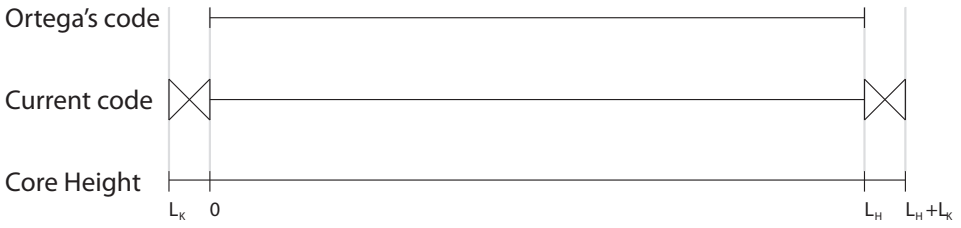

Figure 3.2: In Ortega Gómez's code the constrictions are implemented as boundary conditions at $x = 0$ and $x = L_H$, see eq. (3.3). In the current code the constrictions (shown as a bow tie in the figure) are modelled as an unheated extension of the core with a "wall" friction determined by eq.(3.4)

$$f = \frac{K_i D_H}{L_K} \tag{3.4}$$

In the formula above L_i is the length of the constriction and K_i is the pressure loss coefficient of the restriction and D_H is the hydraulic diameter. The length of the constrictions was set at 0.175 for the HPLWR. This length was chosen because it allowed for about 10 nodes within the constriction which proved, by trial an error, to be necessary to allow the steady state code to converge.

Improving Convergence

Whether or not the problem converges is very sensitive to a number of parameters. First is the initial guess for the inlet mass flux. If it is too low the initial guess results in extremely high temperatures, creating a system difficult to model. Giving an accurate initial guess gets better results, however, based on experience, the best results are obtained if a guess is made which

is slightly less than the expected mass flux. The further the initial guess is from the expected result the longer the computation will take.
Another parameter which is of importance is the pressure drop. If the pressure drop is too low the solution will not converge. It is not clear why the program's convergence depends sensitively on the pressure drop. The stability of the system is, however, independent of the pressure drop as has been shown by Ortega Gómez et al.[18]. This means that the pressure drop can freely be chosen without affecting the NSB which is being investigated. In general increasing the pressure drop will improve the code's convergence.
The main algorithm used is UMFPACK which is an acronym for Unsymmetric MultiFrontal PACKage. It is a solving method often used for unsymmetric sparse systems and is the most stable algorithm available in COMSOL to solve this system. There are a number of parameters which can be adjusted to improve the convergence of the solution. For most stability calculations the standard settings will provide adequate results. If however there are problems converging the solution, the damping factor parameters need to be adjusted. The standard minimum damping factor is set to 10^{-4}, however, marking the system as a highly non-linear problem sets the minimum damping factor to 10^{-8} and the initial damping factor to 10^{-4}. The "highly non-linear" settings will usually help the system to converge. If a large number of simulations need to be solved (for example in a stability plane calculation) it pays to manually set the initial damping factor to 1 and the minimum damping factor 10^{-8}. This decreases the necessary computation time.

3.2.2 Finding the Neutral Stability Boundary (NSB)

The steady state solver produces a `.mat` file which is required for the NSB solver. The `.mat` contains a `fem` structures. This is a structure which COMSOL natively uses to store all the information on the system, including the system of equations, constant, boundary conditions etc. The `.mat` file also contains information on the fluid which was used in the steady state solver. The NSB solver uses the steady state solution provided by the steady state solver as an initial operational point[1] from which to calculate new operational points.
Once the initial state has been loaded a calculation of the eigenvalues of the steady state is made. The heating power is then increased and a new steady state calculation is performed followed by an eigenvalue calculation. This is done until the eigenvalue changes sign, which signals that the NSB has been crossed after which the program makes an educated guess of the power of the operational point on the NSB (see Fig. 3.4. Once the NSB has been crossed the program will usually find the NSB within one to two iterations.

[1] An operational point is a steady state determined by the subcooling number and the dimensionless enthalpy jump

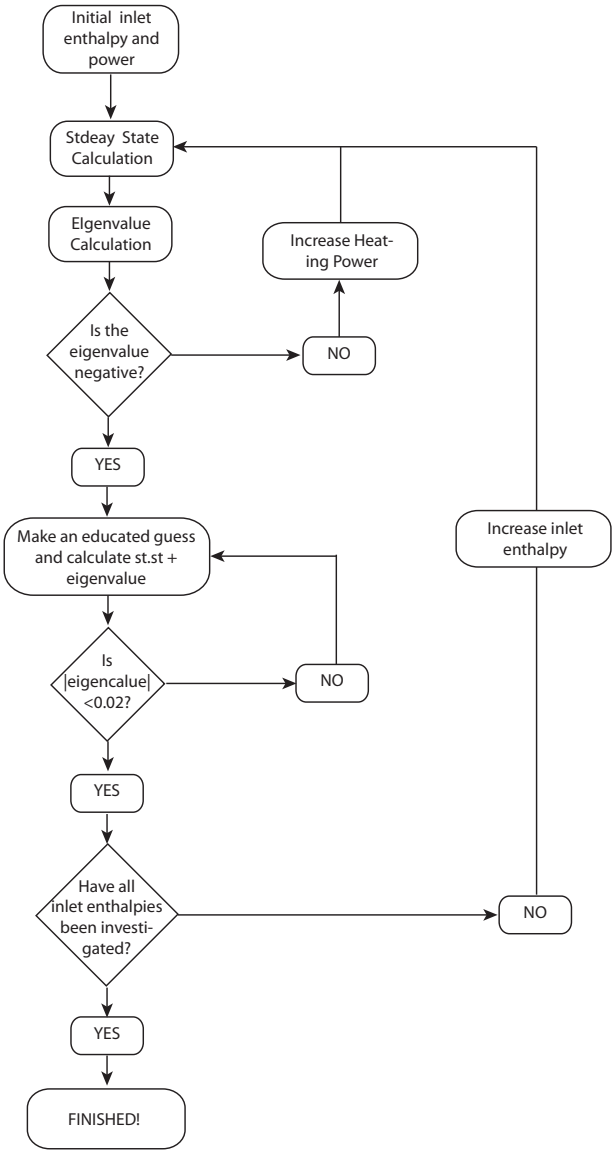

Figure 3.3: Schematic representation of the program developed to find the NSB line of a system.

This procedure is then repeated untill all required inlet enthalpies have been investigated. The scheme used to find the NSB is represented schematically in Fig. 3.3.

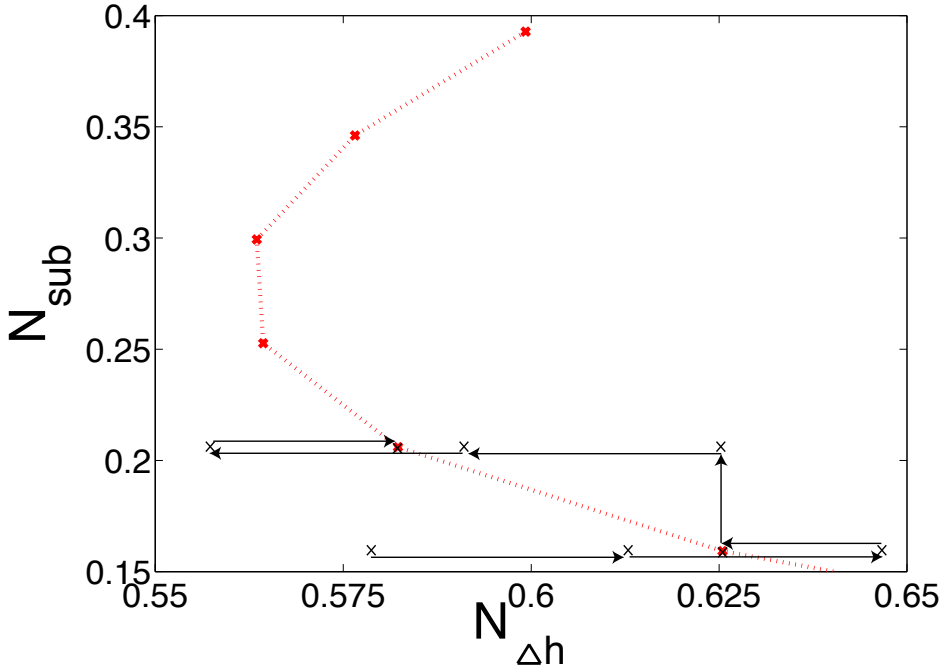

Figure 3.4: The results produced by the current code show similar results to Ortega Gómez et al.[18]. There is a systematic difference in pseudo-subcooling number, which can be explained by a difference in choice of pseudo-critical enthalpy.

3.3 Validation of Steady State Solver

To validate the steady state solver a number of simulations were carried out using the same parameters in the steady state solver and in a Maple script. The Maple script was developed as a validation of the steady state code. This specific example was calculated using the HPLWR system with an inlet enthalpy of $H_{in} = 1.4MJ.kg^{-1}$, a pressure drop of $p_{drop} = -300kPa$ and a power of $q_w = 800MW.m^{-3}$, which resulted in a mass flux of $G = 4962kg.m^{-3}$ in the steady state code. The Maple script must have a mass flux as an input and calculates the corresponding pressure drop which was $298.55kPa$. This differs from the COMSOL steady state calculation by less than 0.5%. The difference can be explained by the way in which the density is defined in the two scripts: COMSOL uses a spline[2] while Maple uses a

[2]A spline is a function composed of multiple polynomials defined on set enthalpy intervals

polynomial function[3].
The Maple script was used quite often during this thesis to check whether changes in the COMSOL script were correct. The two scripts never differed by more than 0.75%.

3.4 Benchmarking of the Neutral Stability Boundary Code

To make sure that the NSB code is calculating correct NSB, the code was benchmarked against the results published by Ortega Gómez et al.[18]. In Fig. 3.5 the results from the current code are compared to those published by Ortega Gómez. The results show a close resemblance. The results from the current NSB code show a systematically higher pseudo-subcooling number. This can be explained by the choice of the pseudo-critical point. If a different pseudo-critical point is chosen the subcooling number will be different. In this case the pseudo-critical enthalpy used by Ortega Gómez is slightly lower than the one used in the current code. The deviation is about 4% of the pseudo-critical enthalpy. The stability code gives the similar results to the results published by Ortage Gómez et al. [18]

3.5 Mesh Dependence

Since a numerical code needs to work with discreet elements, the core is divided into a number of mesh elements. The size of mesh elements can be of influence to the performance of the COMSOL code, if the mesh is too coarse there will be an error in the results. If it is too dense it will take long to calculate. In Fig. 3.6 it can be seen that the program is insensitive to the mesh size uptill at least a mesh size of $0.03m$ and a relatively large mesh size can be chosen. The standard mesh size for HPLWR calculations was $0.00875m$, which is well below the limit. For systems with a different core size the mesh size has been scaled with the length of the core, thereby keeping the number of mesh elements in the simulation constant.

3.6 Sensitivity of stability to fluid properties

Previous research [12, 19] has shown that the NSB is very sensitive to the EOS. This means that care must be taken with the implementation of the EOS (i.e. density and viscosity). The two properties, density and viscosity of the EOS, need to be implemented as a function of enthalpy in the steady

[3]COMSOL has difficulties with high degree polynomials and Maple works with polynomials better than with a spline

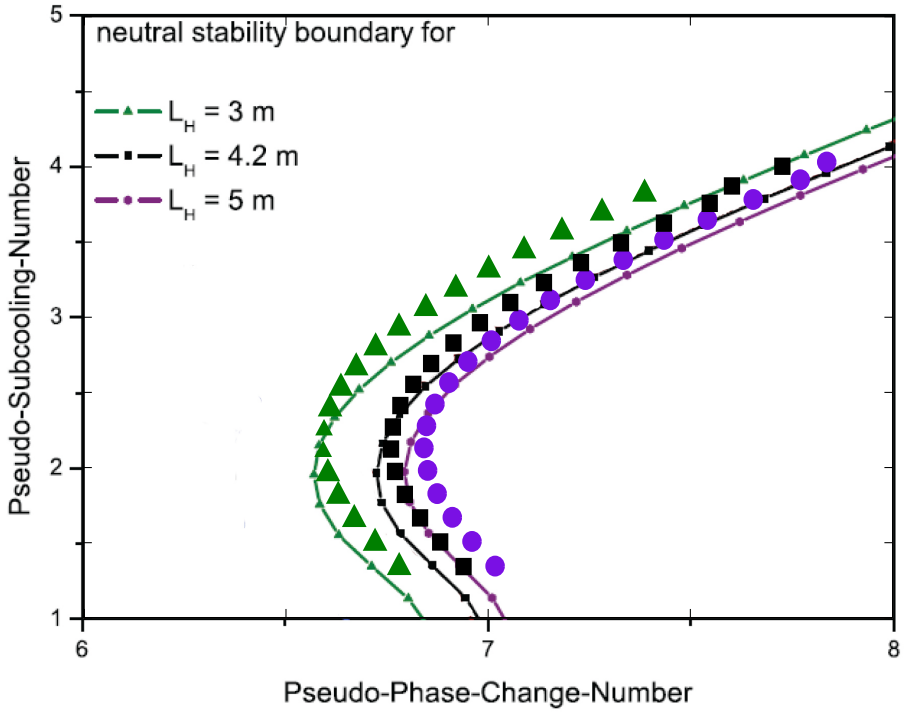

Figure 3.5: The results for Ortega Gómez are connected by a line while the results from the current code use the same but much larger symbols, which are not connected. The results produced by the current code show similar results to Ortega Gómez et al.[18]. There is a systematic difference in pseudo-subcooling number, which can be explained by a difference in choice of pseudo-critical enthalpy.

state code. These properties can be found in a database provided by NIST (National Institute for Science and Technology)[15] . The data points which can be extracted can be used to create the required density and viscosity functions. This section will explain how the density and viscosity functions were created, what other options were available and why the chosen option was considered the best.

Cubic splines and polynomials

The data points from the database can be modelled in a number of ways with the MATLAB curve fitting tool. The most promising curve fitting models were the polynomial fit and the cubic spline. Both result in a continuous curve as well as a continuous derivative with respect to enthalpy, which is important for the conservation of mass (see eq. (2.3)). The main difference is that the cubic spline ensures that the curve fits the data exactly while the polynomial fit uses a least squares method to determine the coefficients of the polynomial, which does not necessarily result in an exact fit with the data points.

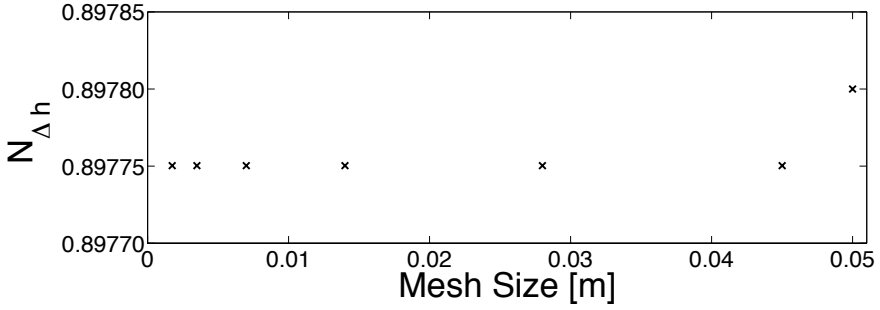

Figure 3.6: The dimensionless enthalpy jump number $N_{\Delta h}$ of the NSB at a subcooling number of $N_{sub} = 0.4891$ for a number of different mesh sizes in the HPLWR system.

In a cubic spline the data points are called "knots". The two fitting models can be applied to the viscosity and density data from the database to investigate the effect of modelling choices on the stability of the system.
The accuracy of the polynomial fit is mainly influenced by the degree of the polynomial used. The accuracy of the cubic spline is influenced by the number of knots used to define the spline. Increased accuracy however results in increased computation time. By looking at the accuracy and necessary computation time of the different fits a choice can be made. To compare the accuracy of different fits both the steady state calculation and neutral stability line calculation are compared.

Density

The description of the density in terms of enthalpy is important to all three conservation equations. The derivative of density with respect to enthalpy is necessary for the equation of mass (see eq. (2.3)). The derivative of density with respect to enthalpy is, however, not given in the database and needs to be calculated. If a polynomial fit is used this calculation is trivial. For the cubic spline the derivative is calculated at each knot (datapoint) of the cubic spline. The derivative of a knot is calculated by retrieving two extra data points, which are as close as possible to the knot. One datapoint at a slightly lower enthalpy and one datapoint at slightly higher enthalpy. The gradient between these points is taken as the derivative of the knot. This method gives a very accurate derivative of the density with respect to enthalpy.
To evaluate the different curve fitting methods the steady state mass fluxes were compared to spot any significant deviation. All the curve fitting methods which calculated correct mass fluxes were then used to calculate a NSB's. This will expose any curve fit which does not accurately model the density

of the cooling fluid. The curve fitting methods which were investigated were:

- cubic spline with 30, 60, 120 and 200 knots at regular intervals
- cubic spline with 33 knots chosen for optimal performance
- polynomial fit of 5^{th} degree

The 5^{th} degree polynomial was chosen because implementing higher degree polynomials prevented the steady state solver form converging. In table 3.1 it can be seen that the polynomial causes a significantly different steady state value of the mass flux and therefore it was discarded as an option. This leaves the four regularly spaced cubic splines and the "optimal" cubic spline.
The optimal cubic spline is not defined by regularly spaced knots with a fixed Δh between each knot. Instead the knots are closer to each other around the pseudo-critical point, since this is where the properties show the greatest change. Visa versa, enthalpies further removed from the pseudo-critical point the spacing Δh is larger to reduce the total number of knots used and thus improve calculation times. The choice of knots was done manually.

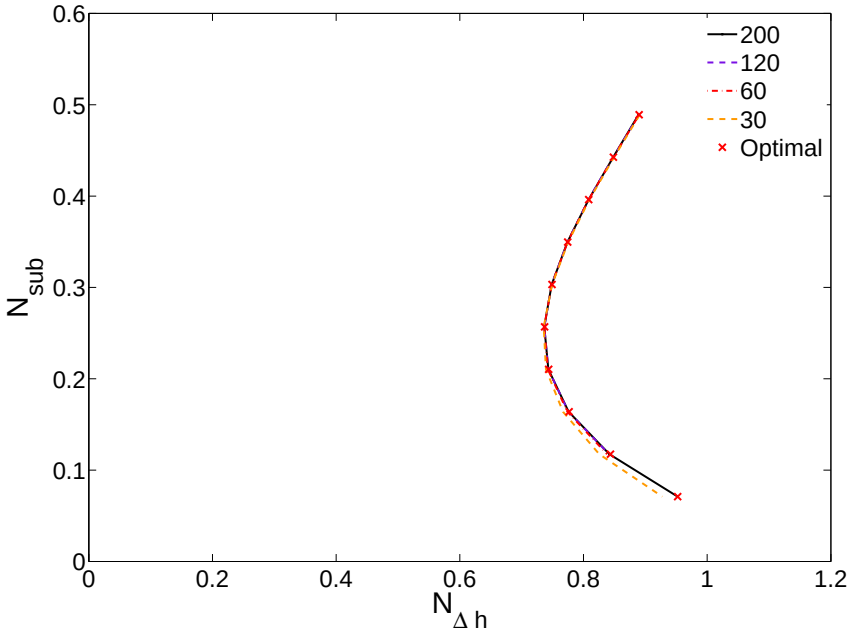

Figure 3.7: Performancs of Freon-23 density splines with 30, 60, 120 and 200 uniformly distributed knots. The optimal spline consists of 30 carefully chosen knots.

Table 3.1: Steady state mass flux values, which show that the mass flux of the 5th degree polynomial deviates from the mass fluxes of the other curve fits. Thus the polynomial is discarded as an option.

Curve Fit	Program	Mass Flux
30 knot cubic spline	Matlab	2876 $kg.m^{-2}.s^{-1}$
200 knot cubic spline	Matlab	2875 $kg.m^{-2}.s^{-1}$
optimal cubic spline	Matlab	2875 $kg.m^{-2}.s^{-1}$
5^{th} degree	Matlab	2971$kg.m^{-2}.s^{-1}$

Table 3.2: Calculation times for different density curve fits. The optimal cubic spline is clearly faster than the 60, 120 and 200 knot splines. The 30 knot spline is slightly faster than the optimal spline but it cannot reproduce the NSB accurately enough as seen in Fig. 3.7

Curve Fit	St.St.	NSB
30 knot cubic spline	8 s	176 s
60 knot cubic spline	12 s	303 s
120 cubic spline	20 s	573 s
200 cubic spline	32 s	-
optimal cubic spline	9 s	192 s

By using the different splines to calculate a NSB, a comparison of their accuracy can be made. The cubic spline using 30 regularly spaced knots deviates significantly from the other fits as can be seen in Fig. 3.7. The three other fits remain close to each other differing by less than $0.001N_{\Delta h}$. This means the three fits can be used to define the density. The use of the optimal spline significantly reduces the computation time needed as can be seen in table 3.2, thus the optimalcubic spline will be used for further calculations.

Viscosity

The other fluid property of importance is the dynamic viscosity. The data is obtained in the same way as for density. A short comparison will be made between a 200 knot cubic spline an optimally chosen 33 knot cubic spline and a 3^{rd} order polynomial based on the 200 data points used for the 200 knot spline. In Fig. 3.8 it can be seen that the accuracy of the calculations is hardly affected by the choice of fit. The calculation time (especially for the steady state times), does diminish significantly (table 3.3). The optimal spline is used in further calculations.

Table 3.3: Performance of viscosity fits for a HPLWR system. The difference in calculation times between the optimal spline and the 3^{rd} order polynomial are quite small.

Curve Fit	St.St.	NSB
200 cs	15 s	-
optimal cs	10 s	175 s
3^{rd} order poly	8 s	176 s

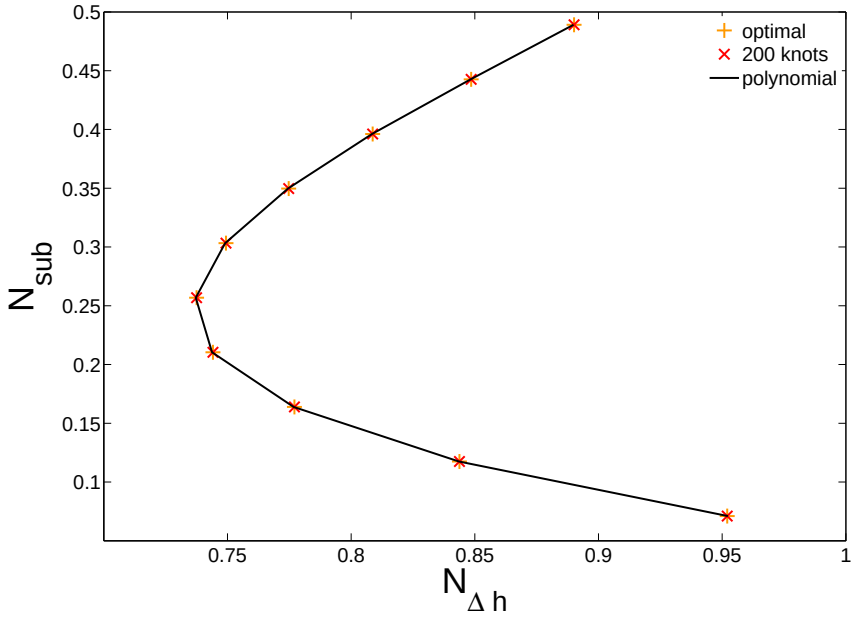

Figure 3.8: Effect of different viscosity fits on the NSB. There is no difference in NSB whether the viscosity is defined using a 200 knot spline, an optimal spline or a polynomial.

3.7 System Pressure Sensitivity

The system pressure is the main parameter determining the equation of state. For the HPLWR the system pressure is planned to be 25 MPa. Within the system there will, however, be a pressure variation in the order of 150kPa which is less than 1% of the system pressure. The pressure variation is, therefore, not expected to significantly alter the equation of state. In Fig. 3.9 three different system pressures have been tested and it can be seen that there is no significant difference. Note that the equation of state does not locally depend on the pressure as this would greatly complicate solving the equations. Instead the system pressure has been changed which leads to

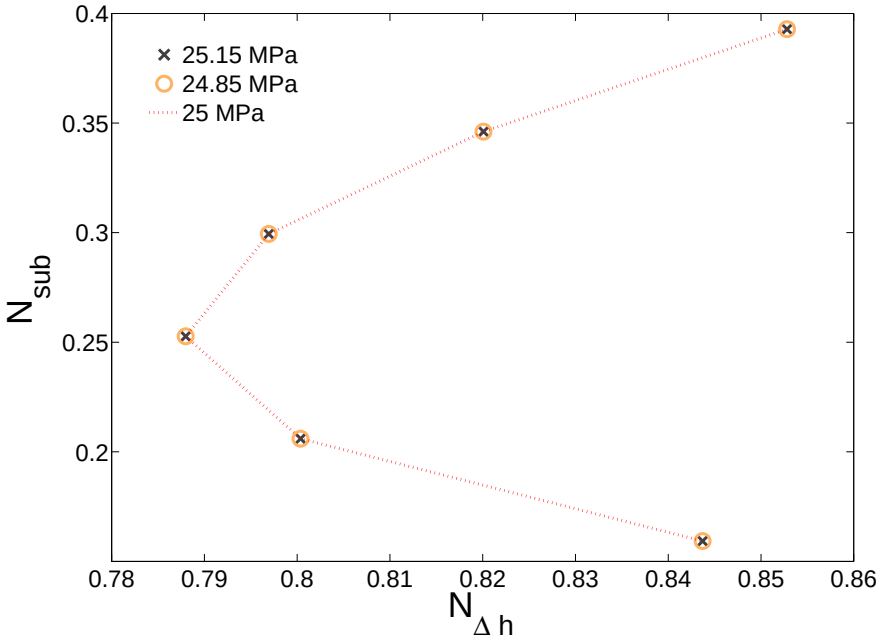

Figure 3.9: Effect of pressure variation on NSB

slightly altered equations of state.

3.8 Summary

The program, which calculates the NSB of the HPLWR, is written using a Matlab script to control COMSOL. The implementation of the governing equations created by Ortega Gómez et al.[18] was used as a starting point to develop the steady state solver. The in- and outlet orifices were modelled in the core instead of incorporating them in the boundary conditions since it was not possible to replicate the previous results using the method described by Ortega Gómez. The result of the steady state calculation is used as the initial condition used to find the NSB of the system. The steady state solver was validated using Maple code and the eigenvalue solver was benchmarked to the results of Ortega Gómez et al.[18]. The implementation for the EOS of the density and viscosity as a function of enthalpy was investigated. A 3^{rd} order polynomial is sufficient to define the viscosity of the cooling fluid, while the density must use a carefully chosen 30-knot optimal spline or a spline with at least 60 uniformly distributed knots. Finally the effect of the pressure drop over the core on the equation of state was seen to have a negligible effect on the resulting NSB.

Chapter 4

Numerical Evaluation of HPLWR Scaling Laws

To investigate the stability of the HPLWR a scaled experimental facility is under developement. The goal of such a facility is to provide experimental data to gain insight into the stability behaviour of super-critical water in the HPLWR. In chapter 2 the scaling laws leading to such a facility (i.e. Delft Light Water Reactor: DeLight). As was explained in section 2.4.3 a number of choices and assumptions were made to achieve the scaling laws used to develop DeLight. These assumptions might lead to a difference in neutral stability boundary (NSB) between the HPLWR and DeLight. Such a gap would limit DeLight's ability to predict the behaviour of the HPLWR. In section 4.1 the NSB of DeLight will be compared to that of the HPLWR. To account for the possible gap between the two NSB's, the scaling of the HPLWR to DeLight, will be broken down into intermediate situations. This will be done in sections 4.3 and 4.4.

4.1 Neutral stability soundaries of DeLight and the HPLWR

DeLight was built to simulate the instability behaviour of the HPLWR. As can be seen in Fig. 4.1 DeLight's NSB resembles that of the HPLWR but there is a difference. The DeLight system is less stable than the HPLWR, except in the lower sub-cooling number region. This can lead to errors in the interpretation of data retrieved from DeLight. To be able to correctly interpret the insights gained by DeLight, the assumptions and choices made leading to the creation of DeLight will be investigated numerically using the steady state and stability code described in the previous chapter.
There are three possible reasons for DeLight's NSB's deviation from the HPLWR's NSB:

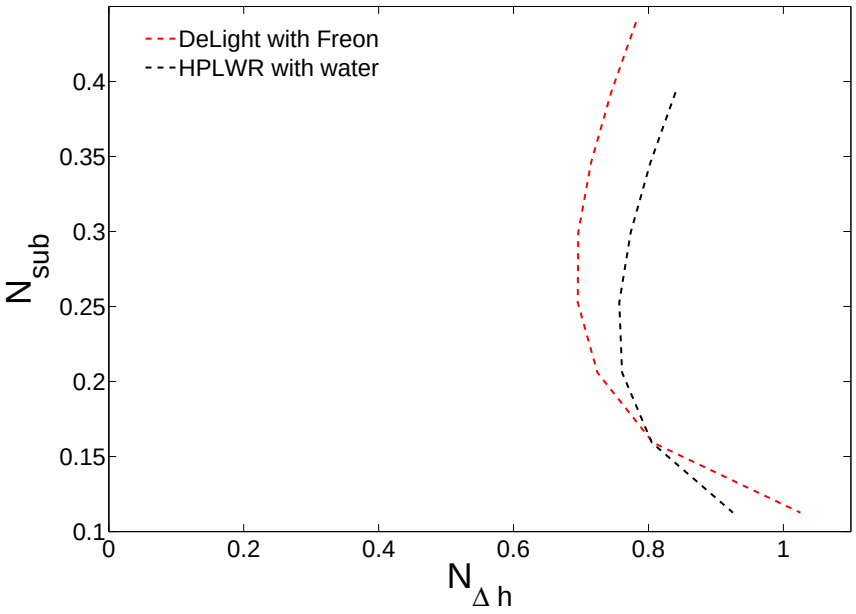

Figure 4.1: NSB of DeLight using Freon-23 as a cooling fluid compared to the single pass core design of the HPLWR with water as the cooling fluid.

- The difference in dimensions between DeLight ($L_C = 0.8m$ and $D_H = 6mm$) as it is being built and the dimensions which follow from the scaling laws used to develop DeLight ($L_C = 0.805m$ and $D_H = 0.5977mm$).
- The use Freon-23 as a scaling fluid
- The assumptions made in order to reduce the friction in DeLight

The first source can be neglected. As can be seen in Fig. 4.2, the NSB of Delight on paper (i.e. according to scaling laws: $L_H = 0.805m$, $D_H = 5.97mm$) and DeLight as built (i.e. actual facility: $L_H = 0.8m$, $D_H = 6mm$) match almost perfectly. Thus they will be treated as the same and refered to as "DeLight".
This leaves two other possible explanations. Freon's dimensionless properties, which do not exactly match those of water, thus possibly accounting for a significant fraction of the gap between the two NSB's. This will be investigated in section 4.3. The other possible source of errors lies in the derivation of the scaling laws for DeLight. During the derivation a number of approximations is made, which could cause a deviation in the NSB. This will be investigated in section 4.4.

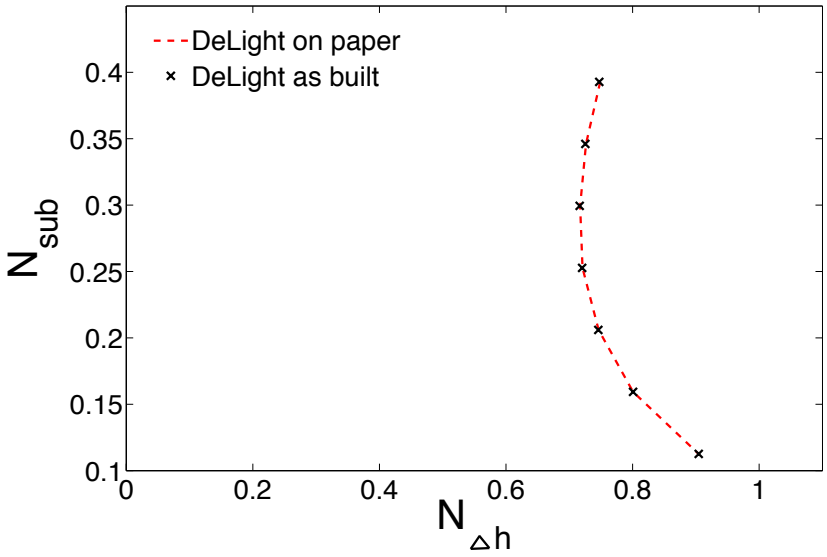

Figure 4.2: The dimensions of DeLight as it is being built are slightly different from the dimensions which follow from the scaling laws. These discrepancies in length and hydraulic diameter do not affect the stability of the system as can be seen above.

4.2 Definitions

To break down the scaling of the HPLWR to DeLight, an artificial system and cooling liquid were created. This allows for two "variables" to be used: the system (i.e. the dimensions and the parameters of the geometry) and the cooling fluid. In Fig. 4.3 the different possible combinations of system and cooling fluid used can be seen. The goal of this chapter is to understand and explain the difference in NSB between the HPLWR and DeLight. To do this a number of fictional intermediate situations have been created to be able to isolate each possible explanation for the gap between the NSB's. In terms of the grid in Fig. 4.3 this means getting from situation 1 to situation 5 via the intermediate situations 2,3 and 4. Once the intermediate situations and how they compare to one another are understood the gap between the NSB of DeLight and that of the HPLWR can be accounted for. The possible situations are schematically shown in Fig. 4.3. A short summary of the definitions of the three systems and three cooling fluids will be given below.

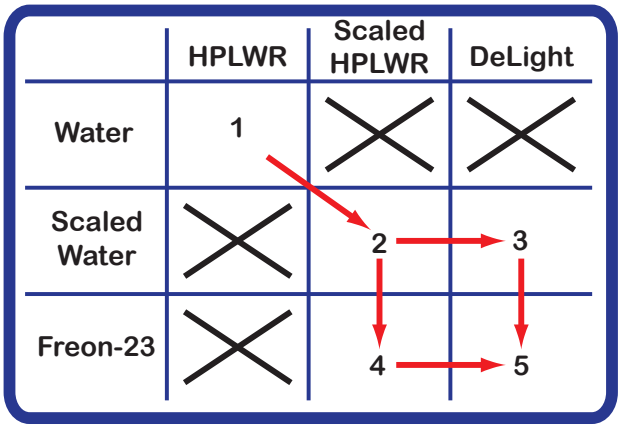

Figure 4.3: Grid showing the system and fluid combinations. Gridspaces marked with an X are not possible. The possible systems are numbered. The numbers will, for clarity, be refered to throughout this chapter. The arrows show the intermediate situations which are investigated.

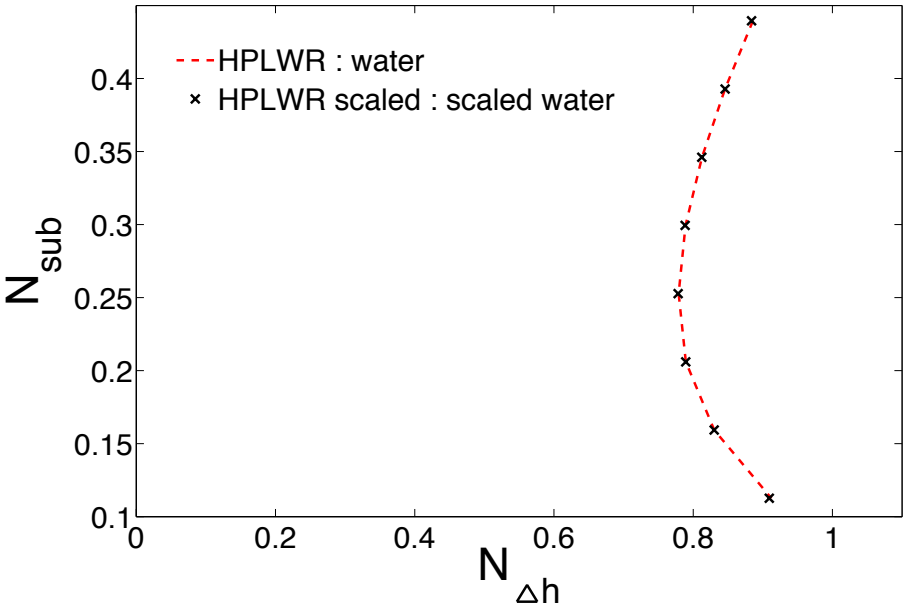

Figure 4.4: The NSB of water in the HPLWR (i.e. grid space 1) is matched exactly by the NSB of scaled water in the scaled HPLWR (i.e. grid space 2). This shows that the scaled HPLWR and scaled water exactly mimic the behavior of the HPLWR cooled by water.

	L_H $[m]$	D_H $[mm]$
HPLWR	4.2	5.62
scaled HPLWR	2.59	3.47
DeLight	0.8	5.97

Table 4.1: The core length and hydraulic diameter of the three systems.

4.2.1 Systems

The so called "scaled HPLWR" follows from the scaling laws, which were derived in section 2.4.3. DeLight and the scaling laws leading to it were also discussed in section 2.4.3 and the HPLWR was introduced in chapter 1. The length of the core and hydraulic diameter of the three systems are compared in table 4.1. The definitions of the three system can be found below:

- HPLWR = The single pass HPLWR core as designed by the HPLWR EU Consortium.
- Scaled HPLWR = HPLWR transformed to the scale of Freon-23, while preserving all dimensionless numbers and therefore the physics of the system.
- DeLight = experimental facility being built at TU Delft, which preserves all dimensionless numbers *except* the Darcy-Weisbach friction factor, which is reduced to allow cooling by natural circulation.

4.2.2 Cooling fluids

By scaling the properties of water using the water to Freon ratios from section 2.4.3, an artificial fluid, which is called "scaled water", is created. The NSB of the "scaled HPLWR" using "scaled water" as a cooling liquid should result in an exact match with that of the HPLWR cooled by water. In Fig. 4.4 it can be seen that this is indeed the case, which validates the correct scaling of the system as well as the fluid. The scaled HPLWR can use either Freon-23 or scaled water as a cooling fluid (see Fig. 4.3). It can thus be used to test the effect of Freon-23 as a scaling fluid while excluding the possible effect of the assumptions used to reduce the friction in DeLight (see section 2.4.3). The most important pseudo-critical properties of the three fluids can be found in table 4.2 and a summary of their definitions can be found below.

- Water = Water at a pressure of $25MPa$.
- Scaled water = Artificial fluid with the same dimensionless properties as water and with the pseudo-critical properties as Freon.
- Freon 23 = Methyl Trifluoride (CHF_3) at a pressure of $5.7MPa$.

	h_{pc} $[MJ.kg^{-1}]$	ρ_{pc} $[kg.m^{-3}]$	μ_{pc} $[\mu Pa.s]$
Water	2.1410	323.0	39,5
Scaled water	0.2869	546.3	25,8
Freon-23	0.2869	546.3	25,8

Table 4.2: Pseudo-critical properites of the three cooling liquids. Note that scaled water and Freon match exactly at the pseudo-critical point but differ at every other enthalpy.

4.3 Influence of the properties of Freon-23

To be able to investigate the effect the properties of Freon-23 have on the stability, other effects need to be excluded. This is done by taking one system (either the scaled HPLWR or DeLight) and changing the cooling fluid. In Fig. 4.3 this corresponds to comparing situation 2 with situation 4 or situation 3 with situation 5. In the following section the properties of Freon-23 will be compared to those of scaled water. This will be followed by an observation of the deviation, which is caused by changing the fluid properties. After which the properties of the fluids will be interchanged to narrow down the source of any gap in NSB's (e.g. using a fluid with the density properties of Freon-23 but the viscosity properties of scaled water).

4.3.1 Differences between the properties of Freon-23 and Water

As mentioned before the dimensionless density ($\rho^*(h^*)$) of water and Freon-23 do not perfectly match. In Fig. 4.5a one can see that they seem to have the largest difference in the lower enthalpy range. When comparing the dimensionless specific volume on the other hand, the largest differences occur in the high enthalpy region, Fig. 4.5c. To get a more balanced view of the differences in density a "normalized" difference function is used, see eq. (4.1). This function's absolute value is invariant to whether calculated using the density or the specific volume. The result of this function can be seen in Fig. 4.5d.

$$||X^*_{H_2O} - X^*_{R-23}|| = \frac{X^*_{H_2O} - X^*_{R-23}}{< X^*_{H_2O} + X^*_{R-23} >}, \tag{4.1}$$

where X^* is any dimensionless property and $<>$ denotes "the average of". The function will mainly be applied to ρ^*. The differences in viscosity between Freon-23 and water are much larger (see Fig. 4.5b). The sensitivity to the EOS and specifically the density have been reported by Jain [13] and Ortega Gómez [19]. No such results have been published regarding viscosity.

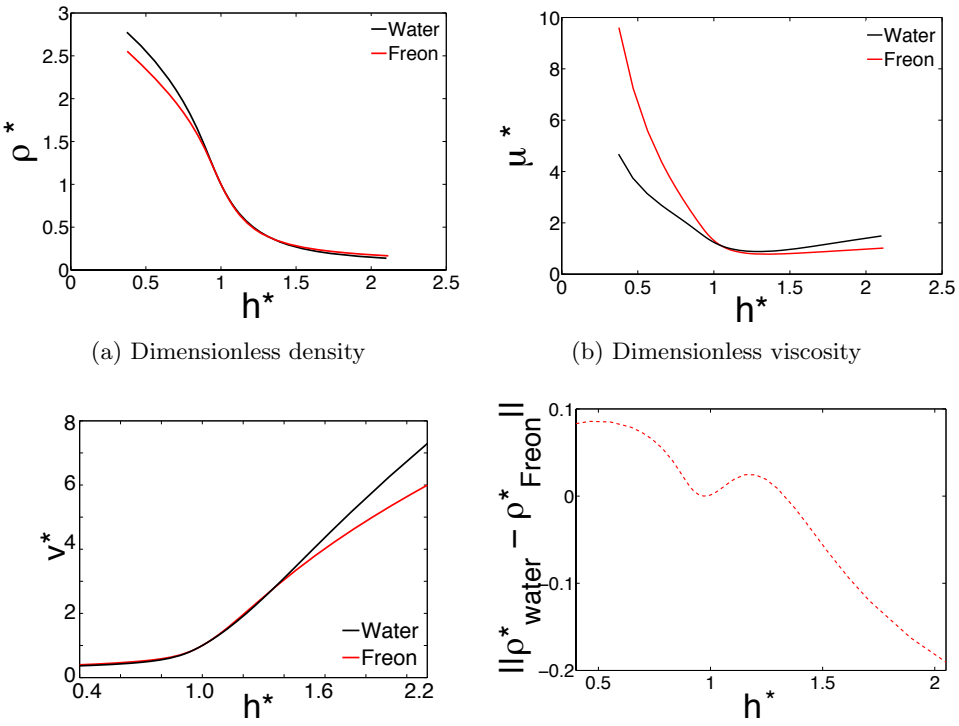

(a) Dimensionless density

(b) Dimensionless viscosity

(c) Dimensionless specific volume

(d) Normalised difference

Figure 4.5: Comparing properties of water to Freon

4.3.2 Stability of Freon-23 compared to the stability of scaled water

To exclude the effect of the assumptions made in the scaling rules, the stability of Freon-23 in DeLight was compared to the stability of scaled water in Delight (i.e. grid situation 3 compared with grid situation 5). The same was done in the scaled HPLWR geometry (i.e. grid 2 compared with grid 4). The resulting NSB's can be seen in Fig. 4.6a and Fig. 4.6b. The maximum difference is about $0.06N_{\Delta h}$, in comparison to the maximum gap between DeLight's NSB and the HPLWR's NSB of $0.09N_{\Delta h}$. This shows that the differences in properties between the two fluids accounts for a large part of the gap between the NSB of DeLight and that of the HPLWR.
Freon-23 also seems to cause the increased stability in the lower sub-cooling numbers, although this is only visible in the DeLight facility and might therefore be caused by the combination of the assumptions made for the scaling of DeLight and using Freon-23 as a scaling fluid. Note that at higher subcooling numbers Freon-23's NSB resembles the NSB of water much more than at lower sub-cooling numbers, especially in the scaled HPLWR geometry.

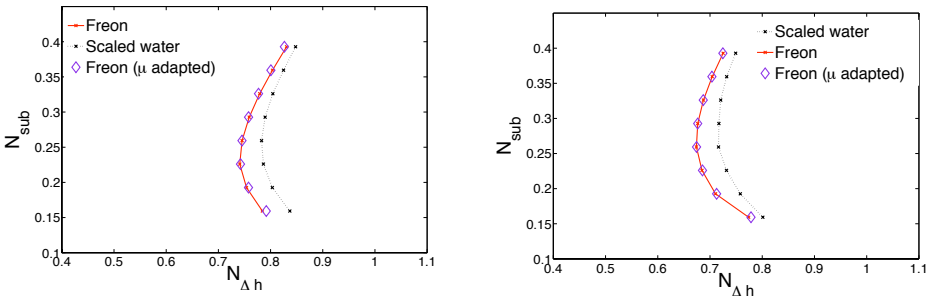

(a) scaled HPLWR (b) DeLight

Figure 4.6: The figures above show two results:
1. Changing the cooling fluid in a system from scaled water to Freon-23 significantly decreases the stability of the system.
2. Artificially adjusting Freon's viscosity to match that of scaled water does not have a significant effect on the NSB.

The difference in NSB caused by Freon-23 can be due to either the viscosity or density of Freon-23, since these are the only two properties of Freon-23 which are used in the numerical code. By seperatly examining the viscosity and density of Freon-23, it can be determined which of the properites is more important in determining the NSB. Viscosity will be examined first after which the effect of density will be investigated.

4.3.3 Viscosity

The dimensionless viscosity of water and Freon do not match well, as can be seen in Fig. 4.5b. This would lead one to expect that the viscosity is responsible for the discrepancies in NSB's. The discrepancy in viscosity, however, does not explain the differences in the stability plane. By changing Freon's viscosity properties artificially to exactly match those of water, the effect of viscosity on the NSB can be evaluated. In Fig. 4.6a and 4.6b it can be seen that there is hardly any difference in the NSB of the system when the viscosity of Freon-23 is artificially adjusted to match that of scaled water. This implies that the difference in viscosity between water and Freon-23 does not account for the difference in NSB observed in Fig. 4.1.
The viscosity affects the system of equations through the Darcy-Weisbach friction factor which is modelled by the explicit relationship developed by Haaland [9]. The effect of viscosity on the friction factor is significant, as shown in Fig. 4.7. The function shown, however, does not take into account the feedback effect which the mass flux has on the friction factor. This can be explained by working out, step by step, the effect of a decrease in viscosity. A drop in viscosity increases the friction factor causing an increase of the pressure drop over the core. If the externally applied pressure drop

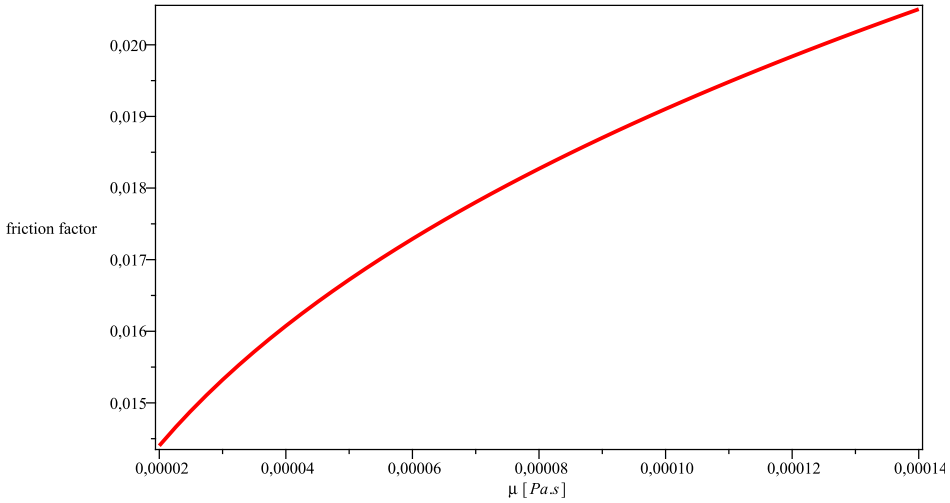

Figure 4.7: Friction factor in water as a function of viscosity with out mass flux feedback, where $D_H = 0.00562[m]$, $\epsilon = 4 \times 10^{-7}[m]$ and $G = 1400[kg.m^{-2}.s^{-1}]$

is fixed the mass flux must decrease, until the pressure drop over the core matches the externally applied pressure drop again. The decreased mass flux in turn causes a lower Reynolds number, which partially or perhaps even fully deminishes the effect of the initial decrease in viscosity.

4.3.4 Density

The analysis of the effect of viscosity reveals that Freon's destabilizing effect on the NSB is solely attributable to its density as a function of enthalpy. To investigate the effect of the density on the stability of the system a number of cooling fluids were designed using the density of Freon-23 and scaled water as a basis. The sets include:

- A set which partially interchanges the properties of Freon-23 and scaled water, these will be called hybrid fluids.
- A set of fluids which were designed using the pseudo-critical point as an anchor and calculating the density function based on an increased gradient $\frac{\partial \rho}{\partial h}$ or an increased normalized difference. These fluids will be referred to as engineered fluids.

By partially interchanging the density, the relative importance of the interchanged section of density on the stability can be evaluated, thereby narrowing down the possible sources of the difference in stability between scaled water and Freon-23.
The engineered fluids were created to see if the properties of scaled water

could be changed in a controlled manner to resemble such that the NSB of scaled water would resemble that of Freon-23. The normalized difference was chosen as a way to adjust density because it is a neutral way of viewing the differences in NSB. In other words whether you calculate changing the normalized difference will reduce the *relative* difference between the density of water and that of Freon-23.

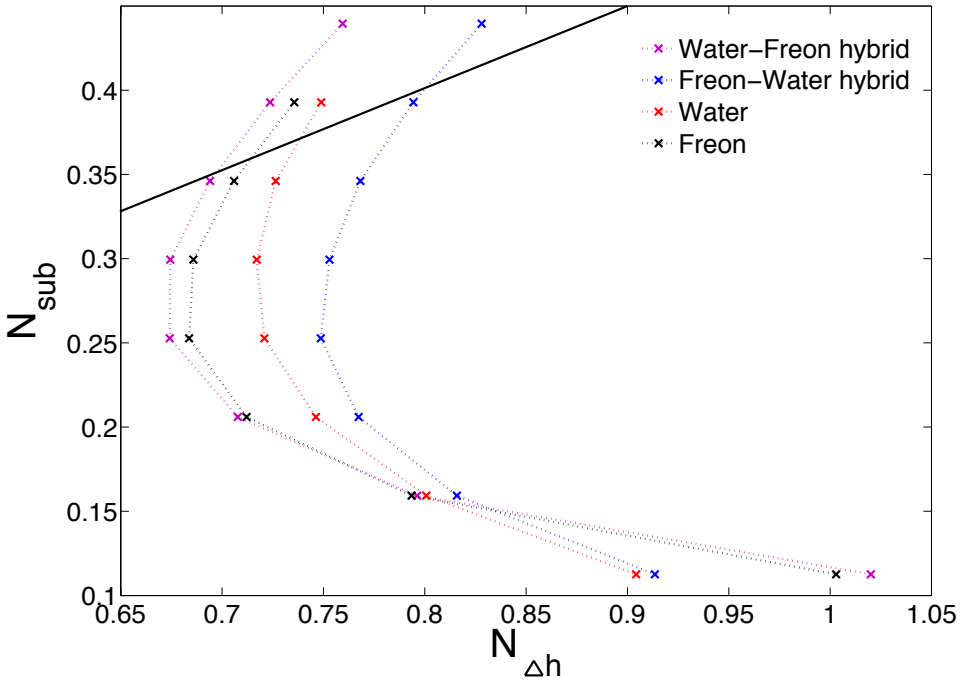

Figure 4.8: NSB's of hybrid fluids compared to NSB's of Freon-23 and water. The black line running through the top left of the figure is the $N_{sub} = \frac{1}{2}N_{\Delta h}$ line. Operational points on this line reach the pseudo-critical enthalpy exactly half-way along the core.

Hybrid fluids

The hybrid fluids were created by dividing the density functions into two parts: enthalpies before the pseudo-critical point (pre-pseudo-critical) and enthalpies after the pseudo-critical point (post-pseudo-critical). Since the dimensionless density of water and Freon-23 match (by definition) at the pseudo-critical point, the pre- and post-pseudo-critical parts of the density functions of water and Freon-23 can be interchanged at will. This leads to two hybrid fluids:

- Freon-water hybrid, density of Freon-23 pre-pseudo-critical point and density of water post-pseudo critical point
- Water-Freon hybrid, density of water pre-pseudo-critical point and density of Freon-23 post-pseudo critical point

The idea behind hybrid fluids is that by interchanging parts of the density properties of Freon-23 with those of scaled water the relative importance of these parts can be evaluated. The post-pseudo-critical point section of the density is expected to be of stronger influence on the NSB than the pre-pseudo-critical point section, due to the larger normalized differences in this section (see Fig. 4.5d). In Fig. 4.8 it can be seen that this is indeed the case. The post-pseudo-critical point section of the hybrid fluids seems to determine whether its NSB resembles that of Freon-23 or water. In other words, the water-Freon hybrid's NSB resembles that of Freon-23 while the Freon-water hybrid's NSB resembles that of water. Fig. 4.8 also shows that the dominance of the post-pseudo-critical point section increases as the sub-cooling number decreases. This can be explained by the enthalpy ranges which are present at these operational points. At lower sub-cooling numbers the inlet enthalpy is relatively close to the pseudo-critical point thus making differences in the post pseudo-critical point section more important for a fixed heat load. It is therefore interesting to look at operational points close to the $N_{sub} = \frac{1}{2}N_{\Delta h}$ line, shown in Fig. 4.8 as a black line. The operational point on this line reach the pseud-critical enthalpy exactly halfway through the core. In the region close to this line the post-pseudo-critical section of the hybrids will dominate less in determining the NSB. The results suggest that it is more important for the scaling fluid to resemble water in the post-pseudo critical point section than in the pre-pseudo-critical point section, which is not the case for Freon-23. The difference between Freon-23 and water are greatest in the post-pseudo-critical enthalpy section, as can be seen in Fig. 4.5d.

Engineered fluids

The engineered fluids are constructed by varying a secondary property (i.e. $\frac{\partial \rho}{\partial h}$ or the normalized difference) of the fluid. The pseudo-critical point is kept the same and the secondary property is used to construct the density as a function of enthalpy. The reason for this investigation is to try to see whether the difference in NSB between Freon and scaled water can be explained by the normalized difference or the difference in $\frac{\partial \rho}{\partial h}$.
The first set of engineered fluids were designed using the normal difference (see eq. (4.1)). The pseudo-critical points of all the fluids in this section are the same, however, the gradient of the normalized difference with respect to the enthalpy was changed to study its effect, see Fig. 4.9a. In Fig. 4.9b one can see that the gradient of the normalized difference only seems to stabilize

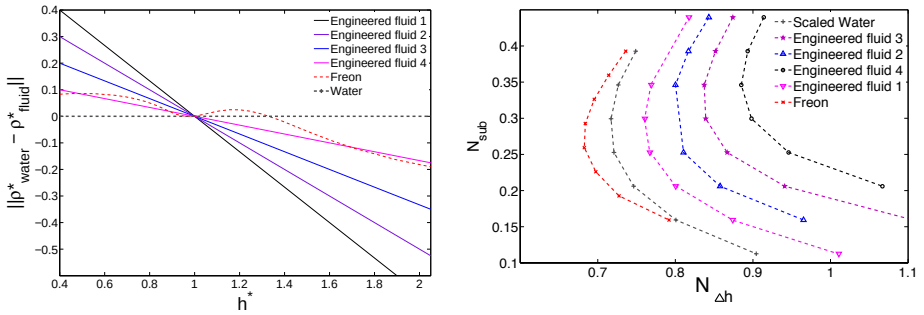

(a) Normalized difference of the four engineered fluids compared with that of Freon and scaled water. The normalized difference is always with respect to scaled water.

(b) NSB's of the four engineered fluids, scaled water and Freon-23

Figure 4.9: On the left the normalized density of the four engineered fluids is compared to scaled water and Freon-23. On the right, the NSB of these four fluids and scaled water is shown.

the system and not destabilize it as Freon-23 does. Engineered fluid 4, seen in Fig. 4.9a, most closely matches the normalized density of Freon-23. Its NSB is, however, more stable than that of scaled water an less stable as is the case for Freon-23. Therefore it seems that the gradient normalized difference does not account for the discrepancy in NSB between scaled water and Freon.

This leads us to our second set of engineered fluids. These fluids have (as with the previous set of engineered fluids) been "anchored" at the pseudo-critical point, but this time the gradient of density with respect to enthalpy $\frac{\partial \rho}{\partial h}$, was varied. In Fig. 4.10a $\frac{\partial \rho}{\partial h}$ of Freon-23 and water is compared to three fluids which were engineered. The resulting NSB's can be seen in Fig. 4.10b. The fluid which is most akin to Freon-23 is the fluid with a $\frac{\partial \rho}{\partial h}$ gradient 0.9 times that of scaled water. This is, however, the fluid with the NSB furthest removed from the NSB of Freon-23. What can be concluded is that a more gradual change in density improves the stability of the system but does not account for the gap between the NSB of scaled water and Freon-23.

4.4 Evaluation of approximations in scaling laws

The DeLight facility was created to be able to replicate the stability properties of the HPLWR. It was also designed to be able to operate using natural circulation as the cooling mechanism. To achieve this the friction in the system needed to be reduced without influencing the stability characteristics of the system [22]. The derivation which justifies reducing the friction in the system without affecting its stability, relies on a number of assumptions.

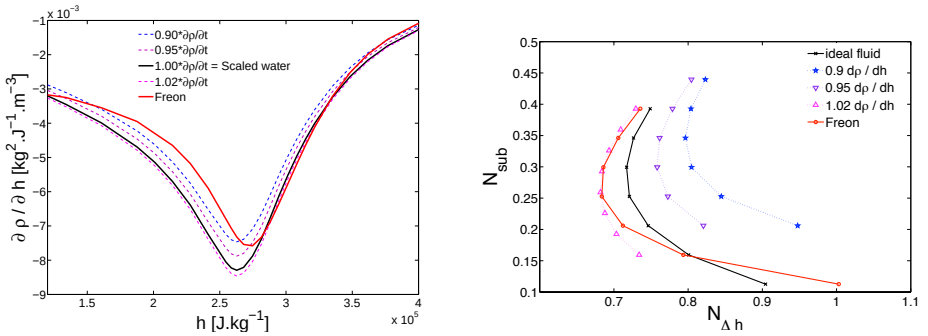

(a) Derivative of density with respect to enthalpy

(b) NSB of the three engineered fluids compared to scaled water

Figure 4.10: On the left the derivative of density with respect to enthalpy of the three engineered fluids can be seen compared to Freon-23 and a scaled version of water. On the right, the NSB of these fluids can be seen.

The three main assumptions are:

- Gravity plays a negligible role in linear stability.
- The inertia of the system ($\frac{\partial G}{\partial t}$) can be ignored in linear stability analysis.
- The EOS can be modelled by a simplified function (see Fig. 4.11), as earlier proposed by Ambrosini [1].

The first assumption is based on a system without a riser and downcomer in which case the gravity term is relatively small. The second assumption ignores the effect of the inertial term which should also be relatively small. The third assumption is that the simplification of the equation of state will not strongly effect the NSB. Since it has already been demonstrated that the stability of the system is extremely sensitive to the equation of state [13, 19], it is expected that this assumption will have the largest effect. In eq. (4.2) the terms which have been neglected to justify reducing the friction have been crossed out. The next three sections will treat each of the assumptions.

$$\cancel{\frac{\partial G}{\partial t}} + \frac{\partial G^2 v}{\partial x} = \cancel{\frac{g}{v}} - \frac{\partial p}{\partial x} - \frac{G^2 v}{2}\left\{\frac{f}{D_H} + \sum_i K_i \delta(x - x_i)\right\} \quad (4.2)$$

Gravity

To evaluate the effect of these assumptions gravity was set to zero and only scaled water was used. The results can be seen in Fig. 4.12. Gravity clearly does not effect the NSB very strongly. Though the zero-gravity case is discernible from the normal gravity case it does not account for a significant

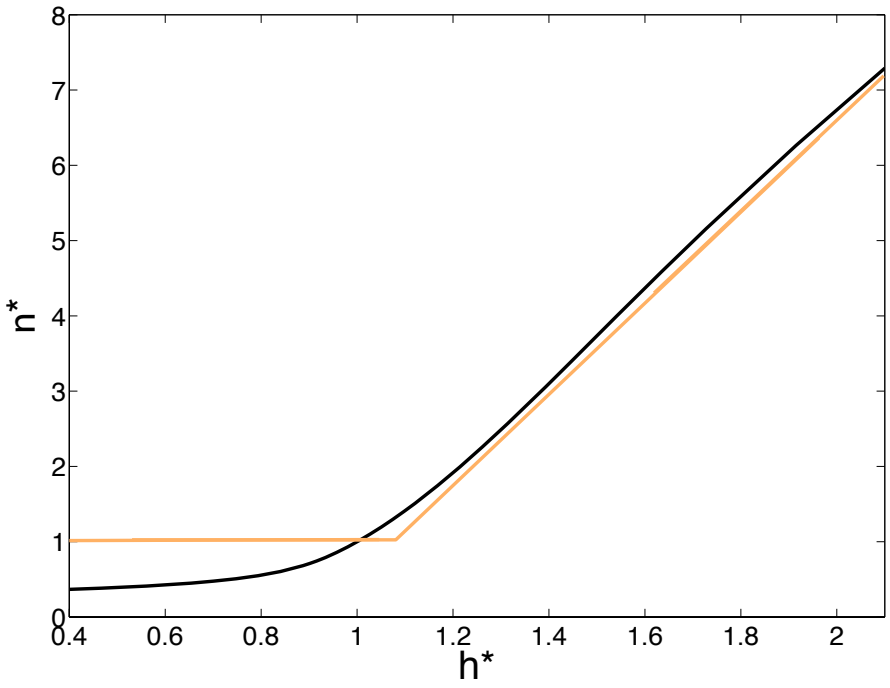

Figure 4.11: The black line is the specific volume of water, which has been approximated by the function shown as an orange line.

difference in NSB between DeLight and the HPLWR.

Inertial term

The inertial term on the other hand has an unexpectedly large effect. Removing it strongly destabilizes the system. Initially this does seems to be obvious since the inertial term adds resistance to any change thus, stabilising it. This is, however, an unexpected result since the size of the inertial term was deemed small enough to neglect when deriving the rules which allow the friction to be reduced. It is not yet understand why this term plays such a strong role. In Fig. 4.13 it can be seen that the effect of neglecting the inertial term in the HPLWR has a much smaller effect. It would thus seem that inertial effect has been exaggerated by the scaling laws leading to DeLight.

Approximation of the equation of state (EOS)

The third assumption is more difficult to investigate since the program has difficulties converging when a sharp change is made in the density profile (i.e. $\frac{\partial \rho}{\partial h}$ is not defined at a certain point). The sollution does not converge even

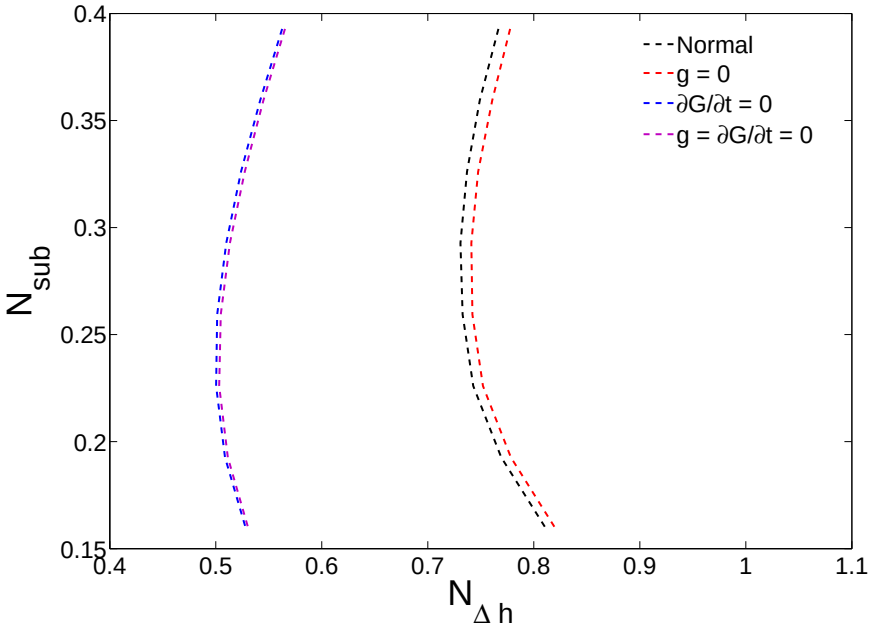

Figure 4.12: Four cases have been simulated in the DeLight geometry: normal, zero-gravity, zero-inertia and finally a combination of zero-gravity and zero-inertia. All of these simulations were performed using scaled water as a cooling fluid to allow direct comparison with the HPLWR.

if the assumption is watered down and the gradients are smoothed out. It was thus impossible to directly investigate the effect of this assumption. The information, which was gained from investigating the other two assumptions, needs to be used to infer the effect of the third one.
In Fig. 4.13 the effect of switching off the inertial term in the HPLWR with water and DeLight using scaled water as a cooling fluid can be seen (i.e. grid 1 and 3 in Fig. 4.3). By eliminating all other possible sources for the difference in NSB it can be concluded that the remaining gap must be caused by the approximation of the specific volume. By using scaled water the effect of Freon-23 is excluded. It is known that gravity has a negligible effect. This leaves two remaining possible causes to account for the difference in NSB between the HPLWR and DeLight: the inertial term and the approximation of the equation of state. If the inertial term is set to 0 in both systems then all possible causes for errors are eliminated except the error due to the approximation of the EOS. In other words the gap between HPLWR $\frac{\partial G}{\partial t} = 0$ and DeLight $\frac{\partial G}{\partial t} = 0$ is solely attributable to the approximation of the EOS. The difference between HPLWR $\frac{\partial G}{\partial t} = 0$ and DeLight $\frac{\partial G}{\partial t} = 0$ is quite large. If, as has been argued above, the difference between these two NSB's is attributable to the approximation of the specific

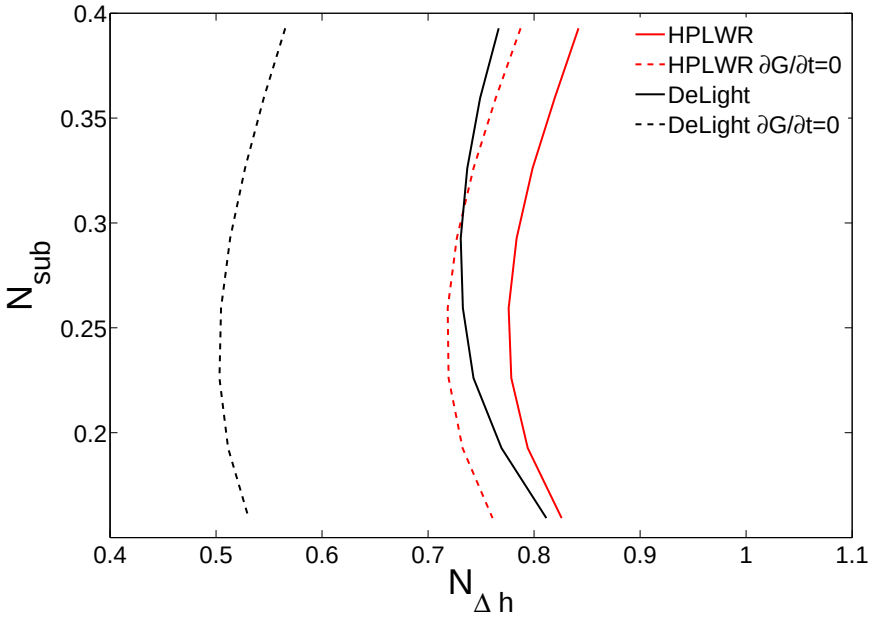

Figure 4.13: DeLight with scaled water and HPLWR with water $g = \frac{\partial G}{\partial t} = 0$. The figure shows that the effect of the inertial term is much smaller in the HPLWR than it is in DeLight. The gap between HPLWR $\frac{\partial G}{\partial t} = 0$ and DeLight $\frac{\partial G}{\partial t} = 0$ is solely attributable to the approximation of the EOS

volume which was made then this assumption is not justified. It should be noted that due to the convergence problems noted above that this is rather "circumstantial" evidence, which should be validated some other way.

4.5 Summary

DeLight will be a slightly less stable system than the HPLWR but will exhibit similar NSB's. The difference in stability is caused by the difference in density between water and Freon-23, as well as by the assumptions made for the scaling laws applied to achieve a reduction in friction in the DeLight system. Both sources contribute in approximately equal parts to the difference in NSB. In future searches for scaling fluids it should be noted that the post-pseudo-critical section is of greater importance than the pre-pseudo-critical section of the fluid density in determining stability. Regarding the assumptions made to justify reducing the friction for DeLight, the approximation of the EOS causes a large discrepancy. Neglecting the inertial term did not have a large effect on the HPLWR, which would justify the assumption. This effect was, however, greatly enlarged in DeLight. Furthermore,

the differences in measurements between the DeLight on paper and DeLight as it has been built are so small that they do no lead to a noticeable change in NSB.

Chapter 5

HPLWR Parameter Investigation

Most research on stability regarding supercritical fluids has focussed on homogeneous heating or has considered the three channels in a three pass core system separately. In this chapter the three pass core as designed in the most recent version of the HPLWR design is modelled. One of the main differences with the single channel core is that gravity is reversed with respect to the flow direction in superheater I, see Fig. 1.2. Furthermore the total length of the channel is triple that of the single pass core which necessitates a much higher pressure drop to accommodate the same core mass flux, let alone the higher mass flux required to be able to be able to accommodate the same power as the single pass core. Additionally the friction in the core can no longer be modelled solely by wall friction but needs to include the pressure drops caused by the connections (mixing plena) between each set of consecutive channels. Finally the three pass-core is designed to operate using a power distribution in which each successive section of the core operates at a lower power. In this chapter the effect of the power distribution, the core length and the intermediate non-wall friction, on the reactor stability will be investigated.

5.1 Core length

Changing the length of the three pass core changes a number of elements in the system but a number of essential things remain the same. The most important parameter which remains constant is the height at which the pseudo-critical temperature is reached relative to the length of the core. This would lead us to assume that changing the length of the core would not significantly affect the NSB. It can be seen in Fig. 5.1 that the effect is small, but there is a clear increase of stability as the length of the core increases.

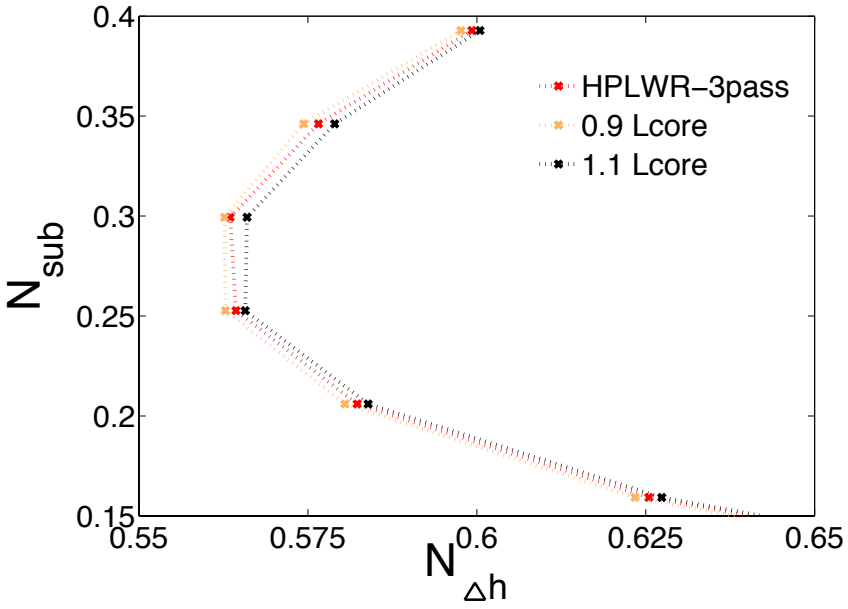

Figure 5.1: Effect of the length of the single pass core on NSB

Ortega Gómez[18] reasons that lengthening the core has a greater effect on the in-phase pressure loss (i.e. pressure drop in higher density region) than on the out-of-phase pressure drop. He argues that the friction term in the dimensionless momentum conservation eq. (2.21) the friction term eq. (5.1) is dominated by the change in specific volume across the core.

$$\frac{f}{D_H^*}\frac{G^{*2}v^*}{2} = \frac{fL_c}{D_H}\frac{G^{*2}v^*}{2} \tag{5.1}$$

The other factors do not vary as much and thus the friction term is smaller in the in-phase region than in the out-of-phase region. Ortega Gómez states that a change in length will therefore have a "relatively" strong effect in the in-phase region. Lengthening the core will, however cause a linear increase of the pressure drop in both regions. Rohde et al.[22] argue that an increase in friction will not affect stability, which contradicts the argument cited by Ortega Gómez. The mechanism behind the stabilisation of the system due to the increase in length is thus not yet clear.

5.2 Comparison of Three-pass Core to Single-Pass Core

The three pass core was designed to be able to cope with the high temperatures reached within the core by allowing for intermediate mixing, thereby limiting the maximum temperature reached in hot-channels. To allow for

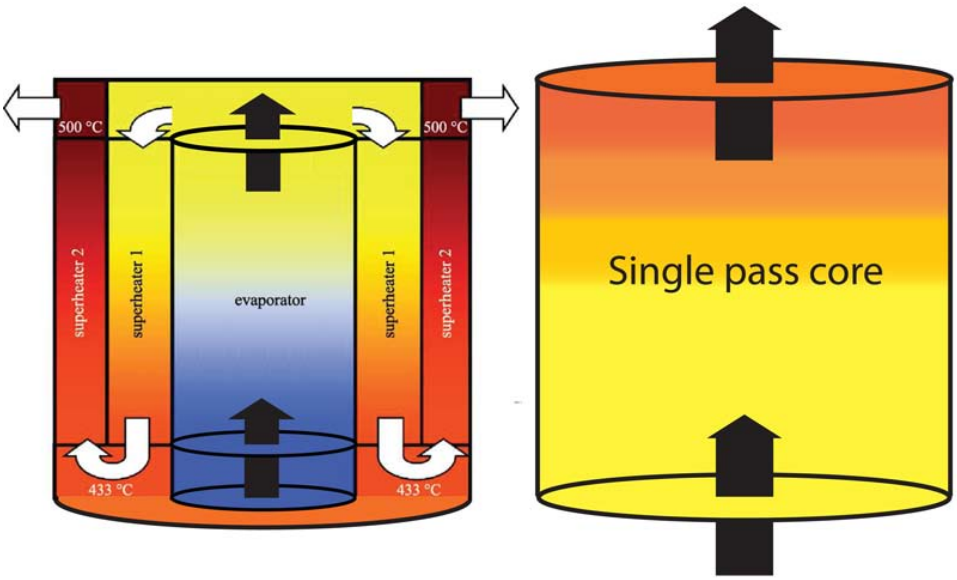

Figure 5.2: Schematic comparison of three pass and single pass core. The cooling fluid in the three pass core only has a third of the cross-sectional area to flow through compared to area available to the cooling fluid in the single pass core. The cooling fluid in the three pass core must cover three times the distance, which the cooling fluid in the single pass core must cover.

this three pass core without changing the outer dimensions of the core and maintaining the power production and inlet enthalpy of the single pass core requires a mass flux which is three times greater mass flux than the mass flux in the single pass core. This can be seen in the following equation:

$$N_{\Delta h} = \frac{P}{h_{pc} G_c A} = \frac{q_w L_c}{h_{pc} G_c}, \tag{5.2}$$

where it should be noted that A is the total cross-sectional area which the fluid can flow through, not the cross-sectional area of a single channel. The length of a three pass core is three times that of a single pass core and the area for the cooling fluid to flow through is one third of the area available in a single pass core (see Fig 5.2). This means that for the three pass core to operate at the same power and dimensionless enthalpy jump the mass flux must be three times greater than in the single pass core. Table 5.1 compares the parameters of a three pass core and a single pass core at the same operational point and the same overall core power output.

The three pass design does not have the same stability characteristics as the single-pass core. Indeed as can be seen in Fig. 5.3 the three-pass core is a more stable system than the single-pass core. There are two main differences

Table 5.1: Parameters for a single and a three pass core at the same operational point and the same power output.

	Single pass	Three pass
q_w	$800MW.m^{-3}$	$800MW.m^{-3}$
A	A_1	$A_3 = \frac{1}{3}A_1$
L_c	4.2m	12.6m
H_{in}	$1.4MJ.kg^{-1}$	$1.4MJ.kg^{-1}$
G	$2032kg.m^{-2}.s^{-1}$	$6096kg.m^{-2}.s^{-1}$

between the three and single pass core which might affect the stability of the system. The first is the increased core length. The cooling fluid in a three pass core has to cover three times the distance the fluid would have to cover in a single pass core. The second difference is that in the middle section (superheater I) gravity is aligned in the same direction as the flow, where as in the single pass core gravity is always in the opposite direction. This could cause the system to become less stable. As was shown in section 4.4 and by Ortega [18] gravity does not have a major effect on the stability of the system and does not explain the difference in stability behaviour. Thus the difference between the NSB's of the single and three pass core must be explained by the increased length of the core. As can be seen in section 5.1 the length of the core can have a stabilising effect on the system. Furthermore Fig. 5.3 shows that doubling the length of the single pass core accounts for much of the increased stability of the three pass core. Therefore the same mechanism which causes a longer single pass core to become more stable also accounts for the increased stability of the three pass core.

5.3 Power distribution

The HPLWR is designed to transfer 54% of its power to the cooling fluid in the evaporator, 30% in superheater 1 and 16% in superheater II. This distribution is a result of the dual function of water in the HPWLR. It acts as both the cooling fluid and the moderator. Thus the power is greatest where the density of the water is greatest: in the evaporator. During the lifetime of a reactor this power distribution may change and it is therefore interesting to simulate different power distributions. Three distinct power distributions are investigated and can be seen in table 5.2.
From previous work in the field of BWR stability analysis ([8, 14]) it is known that increasing the height of the boiling boundary greatly reduces the appearance of density wave oscillations. In other words a boiling boundary higher up in the core increases stability and therefore a top peaked power distribution is more stable than a bottom-peaked distribution [25]. Since supercritical fluids lack a boiling boundary the pseudo-critical point will

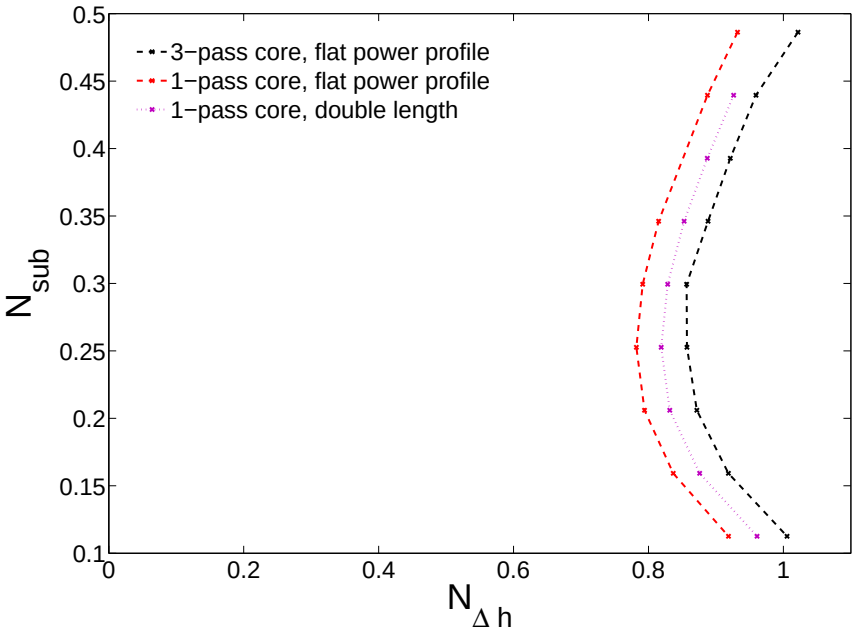

Figure 5.3: Comparison of the NSB of a single-pass core and a three-pass core. Doubling the length of the single pass core shows that the increased length is an important factor in the increased stability of the three pass core.

Table 5.2: Relative distribution of power for 3 different power profiles

Profile	Evaporator	Superheater I	Superheater II
HPLWR	54%	30%	16%
Flat	34%	33%	33%
Inverse	25%	33%	42%

serve as the super-critical equivalent of the boiling boundary. The standard HPLWR power profile will cause the pseudo-critical point to be attained much closer to the inlet than the other two profiles. This would suggest that the normal HPLWR profile is in fact the least stable profile of the three investigated profiles. This is supported by the stability analysis done with the three-pass core model which can be seen in Fig. 5.4.
The inverse power profile is not very realistic when taking the neutronics involved into account. Due to water's function as the neutron moderator the highest power will always be achieved in the region where water has its highest density. By allowing the high density coolant to enter the core on the outside of the core one could create a flatter power profile making the system more stable in the thermo-hydraulic sense of the word. Note that

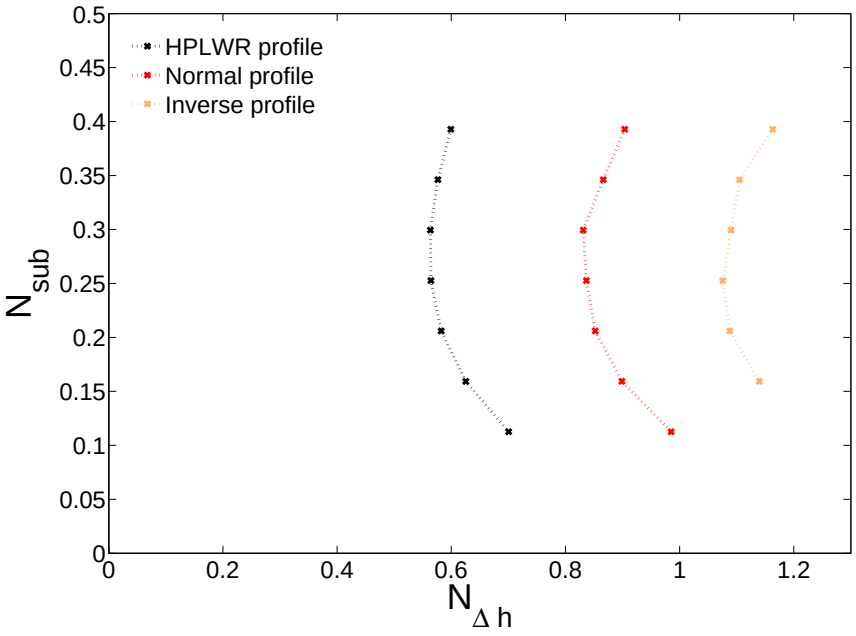

Figure 5.4: Three power distributions were examined: 1. the normal power distribution as planned for the HPLWR, 2. a flat power distribution with each channel contributing an equal amount of power. 3 an inverse power profile, where the superheater II has the highest power output and the evaporator has the smallest (i.e. the inverse of the HPLWR profile)

this, however, would facilitate an increased neutron leakage due to the higher neutron density on the outer boundary of the core. Furthermore it should be noted that at exit of the core the highest possible enthalpy should be achieved as this improves the efficiency of the system. So any redesigning of the system should keep in mind that maintaining a high density throughout a large section of the core will increase the stability, this should result in a reduction of the core exit enthalpy of the cooling fluid. The three power profiles which have been simulated all have the same exit enthalpy and should theoretically achieve the same thermodynamic efficiency.

5.4 Effect of Friction due to Mixing Plena

The three-pass core calls for a number of mixing plena in the system which cause friction and thus a pressure drop within the system. It is known that in- and outlet constrictions can significantly affect the stability of a system. In the previous sections the friction from the mixing plena have been ignored. The question is, what the effect is of intermediate constrictions on the stability of the system.

For the HPLWR design Ortega et al.[19] have shown that the inlet friction causes an increase in stability while an outlet friction imposed on the core causes a decrease in stability. The difference between the inlet and outlet is their relative position to the boiling boundary, or in the case of the HPLWR, to the pseudo-critical point. It is, therefore, expected that the second mixing plenum will always have a destabilizing effect since the pseudo-critical point will in general be reached before this plenum, with the normal HPLWR power distribution. The first mixing plenum, on the other hand, is expected to be destabilising at lower sub-cooling numbers since the pseudo-critical point will be reached before the plenum, while it is expected to be stabilising in the higher sub-cooling number range since in this case it will act as an additional inlet friction. In Fig. 5.5 it can be seen that the effect of the mixing plena does not seem to be dependent on the sub-cooling number. Instead the first mixing plenum consistently makes the system more stable while the second mixing plenum consistently makes the system less stable. The black line indicates the operational points which reach the pseudo-critical point at the first mixing plenum, this would mean that a destabilizing effect would have been expected. The reason for this is might be that the pseudo-critical point is not a good substitute for the boiling boundary and a point with a higher enthalpy should be chosen as the super-critical "boiling boundary". This point would not be reached before the first mixing plane and would explain why friction from the first mixing plenum has a stabilizing effect in all the operational points which were simulated. This explanation would, however, require that the stabilizing effect become less in higher subcooling regions since the effect of the constriction on the in-phase pressure drop would decrease. This effect has not been observed and thus further investigation is required to understand effect of the intermediate mixing plena.

5.5 System pressure

Increasing the system pressure changes the equation of state of water. In section 3.7 the effect of the local pressure drop on the equation of state was investigated and found to be negligible. If, however, the system pressure is changed by a significant amount ($\sim 1MPa$), it is expected to have a significant effect on the NSB of the system. If such a large change in system pressure is applied, the pseudo-critical point is achieved at a higher enthalpy and the derivative of density with respect to enthalpy decreases. This implies that the variation in density along the length of the core is smaller. Which in turn will diminish the feedback effect in the density wave oscillation, therefore making the system more stable. This effect can be observed in Fig. 5.6, in which the largest system pressure clearly causes a more stable system. If the system pressure is high enough it could be possible to make

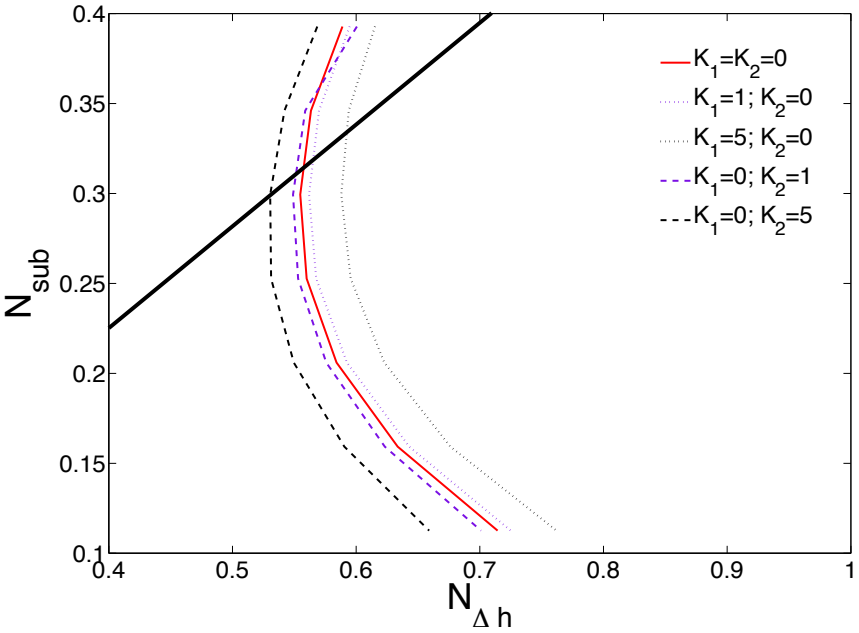

Figure 5.5: Effect of the intermediate mixing plena on the NSB of the three pass-core. A normal HPLWR power profile is used. The pressure loss coefficients of the mixing plena (K_1 and K_2), which were simulated are similar to those used by Ortega Gómez[18] to simulate the inlet and exit constrictions. K_1 is the pressure loss coefficient of the first mixing plenum and K_2 that of the second mixing plenum. The black line marks all the operational points which reach the pseudo-critical enthalpy at the first mixing plenum.

the system extremely stable. The maximum exit temperature (620°C) could even be achieved without reaching the pseudo-critical enthalpy. This would not only create a more stable thermo-hydraulic system, it would also allow for a flat power profile, increasing stabilty even more. The down side is that the material and RPV requirements would make the system much more expensive. Also an important negative feedback (void-reactivity) in the fission reaction would not be as effective.

5.6 Summary

The three-pass core design of the HPLWR without the mixing plena is more stable than the single pass core design due to the increased length of the core. The mechanism behind this stabilization is not yet known. Furthermore, the peak power should be close to the exit of the reactor to create a more stable system, although this may be hard to achieve since a lower density will

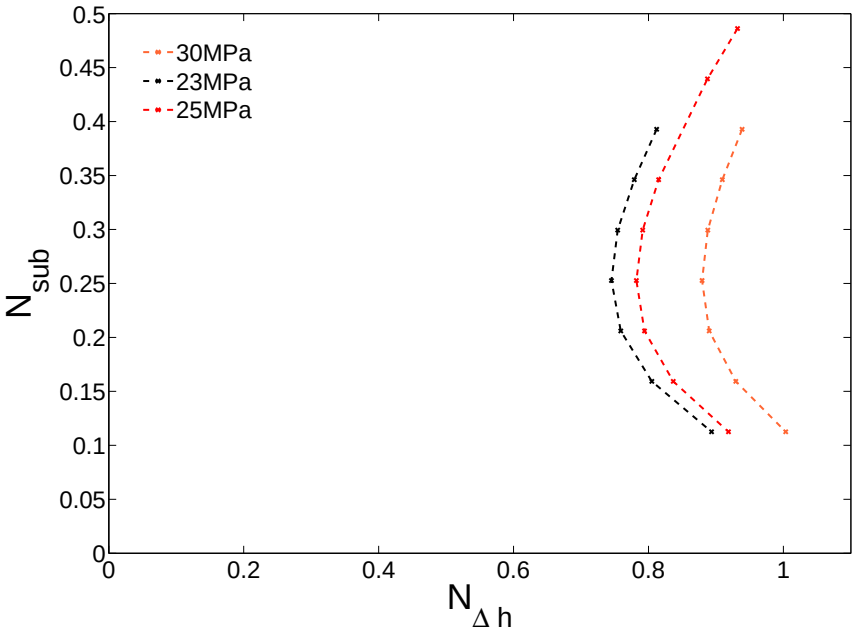

Figure 5.6: Effect of the system pressure on the NSB of a three-pass core.

negatively affect the fission rate and thus reduce the power. The effect of the mixing plena on stability is not dependent on the sub-cooling number, which was not expected a priori. The first mixing plenum stabilises the system while the second mixing plenum destabilises it for all operational points investigated. Finally, a higher system pressure decreases $\frac{\partial \rho}{\partial h}$, making the system more stable. A higher system pressure will, however, decrease the negative void reactivity feedback which is necessary to keep a number of light water nuclear reactor designs inherently stable.

Chapter 6

Discussion and Conclusion

This thesis project has three interlinked goals. These are to create a code able to simulate a supercritical fluid system and find the neutral stability boundary of this system. The second goal is to use this code to evaluate the scaled HPLWR facility, DeLight. The third goal is to investigate a number of HPLWR design parameters which had not yet been examined.

6.1 Choosing dimensionless numbers for the stability plane

To be able to compare different systems a stability plane is used. Its axes are determined by the dimensionless numbers which are being varied. The dimensionless numbers developed by Ortega Gómez et al.[18] for the stability plane, are difficult to reason with because the pseudo-subcooling number cannot be varied independently of the pseudo-phase-change number. Iso-power and iso-inlet enthalpy lines form a curved lattice in the stability plane making it difficult to interpret. Therefore it is suggested that the subcooling number N_{sub} and dimesionless enthalpy jump $N_{\Delta h}$ (first used by Rohde et al.[22] be used in future work regarding heated supercritical channel problems.

6.2 Creation of a neutral stability boundary code

The code, which was created during this project and based on code by Ortega Gómez et al.[19], successfully reproduced the results published by Ortega Gómez et al. The code uses a different way of modelling the inlet and outlet constrictions compared to the original code supplied. The original in- and outlet implementation present in the code which was given to the TU Delft was not able to reproduce Ortega Gómez et al.'s results. By implementing the inlet and outlet constrictions as an unheated part of the core they are

more intuitive to work with and the program was able to replicate the results of previous research.
The stability boundary code was benchmarked to the results published by Ortega Gómez[18]. There was a slight difference in the results, which can be explained by a difference of upto 4% in the choice of the pseudo-critical point. The steady state code was validated using a script written in Maple. This resulted in difference of less than 0.6% in the calculation of the mass flux of the system, which can be attributed to the different way in which the density is implemented in COMSOL and Maple.
The code has been tested for its sensitivity to the implementation of cooling fluid properties (viscosity and density). The results of this were that special attention must be paid to the implementation of the density function as this has a strong influence on the computation time and accuracy of the results. The best results were achieved with a 30 manually chosen knots which was able to simulate a stability boundary comparable to a 200 knot spline, while having a computation time similar to a normal 30 uniformly distributed knots splin. For the viscosity a 30 knot spline or a 3^{rd} degree polynomial is sufficient. Furthermore the pressure variation within the core does not need to be taken into account in the EOS, even though the stability of the system depends sensitively on the EOS.
The DeLight facility was not yet completed at the time of writing of this thesis and so it was not possible to compare experimental results with results from the code. DeLight can, in the future, be used to improve the code. To be able to correctly compare the experimental setup with the code, the code must be able to simulate a cooling loop (i.e. the beginning and end are connected). Creating a loop in the code is the greatest obstacle preventing a comparison between DeLight and the code and any effort to improve the code should have a loop as its main objective.

6.3 DeLight as a scaled HPLWR

The neutral stability boundary plots achieved for DeLight closely resemble the results from the HPLWR. This means that DeLight can be used to gain valuable insight into the stability behaviour of the HPLWR. There are, however, differences and these should be taken into account when interpreting results from DeLight. The source of these differences lies in the use of Freon-23 as a scaling fluid and the assumptions made in order to arrive at the scaling laws for DeLight.
The difference in viscosity between Freon-23 and water was unimportant for the stability of the system. The difference in stability boundary due to Freon-23 as a scaling fluid is, therefore, solely attributable to the difference in density between the two fluids. The differences in the density in the post pseudo-critical enthalpy range plays a larger role than the pre-pseudo-critical

density. This is presumably due to the change in enthalpy in the core being far greater than the enthalpy required to reach the pseudo-critical enthalpy, thus giving more weight to the post-pseudo-critical densities. A smaller derivative of density with respect to enthalpy was seen to have a stabilizing effect. It does not, however explain the difference in stability boundary between water and Freon-23. The mechanism through which Freon-23 causes a less stable system has not been identified yet. This having been said Freon-23 remains a good scaling fluid.
The assumptions, made in the derivations used to arrive at the scaling laws for DeLight, account for the remaining difference in stability boundary between the HPLWR and DeLight. The effect of gravity is small and, therefore, can be considered a reasonable assumption. The second assumption which neglects the inertial term, however, seems to have a large effect on the location of the stability boundary. It is not clear why this term is so important. The third assumption was expected to be the most critical one: an approximation was made of the equation of state (i.e. the density). Previous research has shown that this strongly effect the stability boundary, which is confirmed by the results from chapter 4. If the inertial term is indeed as important as the results suggest, it is also important to know how this might effect the dynamic behaviour of the system and should be investigated in any further research.
If the simulation of a forced circulation HPLWR had been the sole goal of DeLight then the best way of improving its stability boundary would be to build a facility which cannot operate under natural circulation conditions. This would allow all the dimensionless numbers to be kept constant thereby improving the facility's resemblance to the HPLWR and greatly reduce the difference in stability boundary between the HPLWR and the experimental facility. Although the assumptions made in the derivation of the scaling laws for DeLight might not be entirely justified, Delight manages to replicate the stability of the HPLWR to a large extent and is therefore a good experimental facility to investigate the stability of both a forced and natural circulation cooled HPLWR. The code, which has been developed can help to explain and predict the stability of the HPLWR based on the results from the experimental facility.

6.4 The HPLWR parameter study

A number of design parameters were tested, including the length, power distribution and system pressure of the core. The three pass core was, as expected, more stable than the single pass core, despite the destabilizing effect of the downward flow in the superheater I. The increased stability seems to be due to the stabilizing effect of its increased length.
The power distribution within the core should be concentrated towards the

exit of the core (i.e. top-peaked power distribution). This allows the pseudo-critical point to be reached further along the core, thereby stabilizing the system. This is, however, difficult to achieve as the highest power density is achieved at the lowest enthalpies due to water's moderator function in the reactor. By increasing the amount of water which is diverted from the downcomer into the core, the power distribution could be further altered to result in a more stable system. Alternative designs such as the one suggested above should be investigated if the thermo-hydraulic stability should become a limiting factor in the construction of a HPLWR.

The mixing plena's effect on the stability of the system was independent of the subcooling number. It is known that the density wave oscillation depends on the boiling boundary location in BWR's and a similar dependance of density wave oscillation on the location of the pseudo-critical point was expected. In the normal HPLWR power distribution the pseudo-critical point is reached before the first mixing plenum at lower subcooling numbers. Therefore the first mixing plenum was expected to have a destabilizing, instead of stabilizing, effect on the system. The reason for this unexpected behavior is unknown and further investigation is recommended.

Increasing the system pressure in the order of $1MPa$ significantly increases the stability of the system. From a strictly thermo-hydraulic point of view a higher system pressure is better for the stability. There are, however, a number of factors which have not been taken into account here. First of all increasing the pressure raises the requirements of the structure and materials of the RPV. Furthermore a higher pressure would diminish the strength of the important void-reactivity feedback since the variation in density would not be as great. Finally, along with the density a number of other properties of water will change and the effect of these changes should be carefully monitored.

Bibliography

[1] Amborisini, W., and Sharabi, M. Dimensionless parameters in stability analysis of heated channels with fluids at supercritical pressures. *Nuclear Engineering and Design 238* (2008), 1917–1929.

[2] Boure, J., Berlges, A., and Tong, L. Review of two-phase flow instability. *Nuclear Engineering and Design*, 25 (1973), 165–192.

[3] Bragt, D. *Analytical Modeling of Boiling Water Reactor Dynamics.* PhD thesis, Delft University Technology, 1998.

[4] Brennen, C. E. *Fundamentals of Multiphase Flow.* Cambridge University Press, 2005. pg 349.

[5] Chatoorgoon, V., Voodi, A., and Fraser, D. The stability boundary for supercritical flow in natural circulation loops part i: h_2o studies. *Nuclear Engineering and Design 235* (2005), 2570–2580.

[6] Cheng, X., and Yang, Y. A point-hydraulics model for flow stability analysis. *Nuclear Engineering and Design 238* (2008), 188–199.

[7] Gen. IV International Forum, U. . A technology roadmap for generation IV nuclear energy systems, December 2002.

[8] Guido, G., and et al. Density-wave oscillations in parallel channels an analytical approach. *Nuclear Engineering and Design 125* (1991).

[9] Haaland, S. Simple and explicit formulas for the friction factor in turbulant flows. *Journal of Fluids and Engineering*, 103 (1983), 89–90.

[10] Ishigai, S. *Steam Power Engineering.* Cambridge University Press, 1999.

[11] Jain, P. K., and Rizwan-uddin. Steady state dynamic analysis of supercritical co_2 natural circulation loop. In *Proceedings of ICONE 14* (2006), International Conference on Nuclear Engineering. Miama USA.

[12] Jain, R. *Thermal-hydraulic Instabilities in Natural Circulation Flow Loops under Supercritical Conditions.* PhD thesis, Universtiy of Wisconsin.

[13] Jain, R., and M.L.Corradini. A linear stability analysis for natural circulation loops under superciritical conditions. *Nuclear Technology 155* (september 2006), 312–323.

[14] Lahey Jr., R., and F.J.Moody. *The Thermal-Hydraulics of a Boiling Water Nuclear Reactor*, 2 ed. American Nuclear Society, 1993. La Grange Illinois USA.

[15] Lemon, E., McLinden, M., and Huber, M. NIST standard reference database 23. database version 7.0, National Institute of Standards and Technology, 2002.

[16] Marcel, C. *Experimental and Numerical Stability Investigations on Natural Circulation Boiling Water Reactors*. PhD thesis, Delft University of Technology, 2007.

[17] March-Leuba, J., and Rey, J. Coupled thermohydraulic-neutronic instabilities in boiling water nuclear reactors: A review of the state of the art. *Nuclear Engineering and Design 145* (1993), 97–111.

[18] Ortega Gomez, T. *Stability Analysis of the High Performance Light Water Reactor*. PhD thesis, Forchungnszentrum Karlsruhe, 2008.

[19] Ortega Gomez, T., and Class, A. Stability analysis of a uniformly heated channel with supercrictical water. *Nuclear Engineering and Design 238*, 8 (August 2008), 1930–1939.

[20] Rizwan-Uddin. On density wave oscillation in two-phase flows. *Int. J. Multiphase Flow 20*, 4 (1994), 721–737.

[21] Rohde, M., Marcel, C., Manera, A., van der Hagen, T. v., and Shiralkar, B. Investigating the ESBWR stability with experimental and numerical tools: A comparative study. *Nuclear Engineering and Design* (2008). In press.

[22] Rohde, M., and van der Hagen, T. Downscaling the HPLWR to an experimental facility by using a scaling fluid. In *Conference Proceedings paper no.9* (2009), International Symposium on Supercritical Water-Cooled Reactors. Heidelberg Germany.

[23] Schulenberg, T., Starflinger, J., and Heinecke, J. Three pass core design proposal for a high performance light water reactor. *Progress in Nuclear Energy*, 50 (2008), 526–531.

[24] Squarer, D., Schulenberg, T., Struwe, D., Oka, Y., Bittermann, D., Aksan, N., Maraczy, C., Kyrki-Rajamaki, R., Souyri, A., and Dumaz, P. High performance light water reactor. *Nuclear Engineering and Design*, 221 (2003), 167–180.

[25] Zboray, R. *An Experimental and Modeling Study of Natural-Circulation Boiling Water Reactor Dynamics.* PhD thesis, Delft University of Technology, 2002.

Appendix A

Nomenclature

A.1 Roman Symbols

A	Cross-sectional area of the channel	m^2
D_H	Hydraulic diameter	m
f	Darcy-Weisbach friction factor	$-$
g	Gravity	$m.s^{-2}$
G	Mass flux	$kg.m^{-2}.s^{-1}$
h	Enthalpy	$J.kg^{-1}$
K	Pressure loss coefficient	$-$
L_H	Heated core length	m
$N_{\Delta h}$	Dimensionless enthalpy jump	$-$
N_{Fr}	Froude number	$-$
N_{P-PCH}	Pseudo-phase change number	$-$
N_{sub}	Sub-cooling number	$-$
p	(Local) pressure	$kg.m^{-1}.s^{-2}$
p_{drop}	Externally imposed pressure drop	$kg.m^{-1}.s^{-2}$
P	Power	W
P_H	Heated perimeter	m
q''	Power per unit area of channel wall	$W.m^{-2}$
q_w	Power per unit volume of channel	$W.m^{-3}$
Re	Reynolds number	$-$
t	Time	s
T	Temperature	°K
$\vec{\vec{T}}$	Deviatric stress tensor	$kg.m^{-1}.s^{-2}$
u	Velocity in the x direction	$m.s^{-1}$
$\vec{v}$	3-D velocity vector	$m.s^{-1}$
x	Height/Length	m
X	Scaling law or ratie	$-$

A.2 Greek Symbols

ϵ	Roughness	m
λ	Height at which $h(x) = h_{pc}$	m
μ	Dynamic viscosity	$Pa.s$
ν	Specific volume of a fluid	$m^3.kg^{-1}$
π	Dynamic pressure	$kg.m^{-1}.s^{-2}$
ρ	Density of a fluid	$kg.m^{-3}$

A.3 Sub- and Superscripts

*	Dimensionless
c	Core
f	Fluid phase
g	Gaseous phase
in	At channel inlet
pc	Pseudo-critical
out	At channel outlet

A.4 Acronyms

BWR	Boiling Water Reactor
DeLight	Delft Light water reactor
DWO	Density Wave Oscillation
EOS	Equation of state
HPLWR	High Performance Light Water Reactor
NSB	Neutral Stability Boundary
RPV	Reactor Pressure Vessel

Appendix B

Short User's Guide

B.1 Creating splines

The program requires four splines, density, inlet density, derivative of density with respect to enthalpy and dynamic viscosity. The program `spline_v2.m` will create these splines. It requires two vectors as input, for example: `spline_v2(h,rho)` will create two character strings called `funccomsol` and `funcmatlab` which describe density as a function of enthalpy. The `funccomsol` can be called in the Matlab command prompt and then coppied into the program `HPLWR_v4c.m`. The `funcmatlab`, can be used to check the created spline in Matlab and if needed manipulate the spline. The inlet density spline needs to be defined in terms of `Hin` and not in terms of `H`. This can be doen by first creating the density spline and then copying the `funccomsol` character string into a simple text editor and automatically replacing `H` with `Hin`.

B.2 The steady state solver

The steady state solver `HPLWR_4c.m` has a number o choice menu's which automatically configure the fluid to be used in the simulation as well as the system in which it is to be configured. Since the program was created before the terminology used in this thesis was fully developed a number of terms will be unfamiliat to the user. The ideal scaling fluid refers to a scaled version of water used to perform a number of tests and investigations, mainly in chapter 4. If Freon or scaled water are chosen as the fluid another menu pop's up. This one requests the geometry/system to be used. The three choices are called ideal scaling, ideal setup and setup. The ideal scaling is a scaled version of the HPLWR in which all dimensionless numbers are conserved. The ideal setup is the scaled version of the HPLWR in which natural circulation is possible. The setup refers to the DeLight facility.
There are a number of parameters which can be chosen. Remember that the

pressure drop `Pdrop` must always be negative. Furthermore the initial guess for the mass flux `Gin` significantly affects the time needed for the problem to converge.

B.3 The NSB solver

The NSB solver `stabline_v4.m` is used for the singel pass core simulations. For the three pass core simulations `stability_three.m` must be used. The difference between the two programs lies in the way in which the constants are defined. In the single pass core program these are defined by: `fem.const{i}`. While in the three pass core they are defined by: `fem.const.Hin` or `fem.const.Pdrop` etc. The program can be fine tuned mainly by defining the number of steps `Hin` must make in scaning the stability plane. Also the initial NSB search can be fine tuned so that the search starts close to the NSB. Note that is must always start on the stable side of the NSB.

Appendix C

Absence of Ledinegg Instabilities

The Ledinegg instability does not occur in the forced flow HPLWR system. This can be shown using a 3D-plot of power vs. mass flux vs. imposed pressure drop. In Fig. C.1 it can be seen that given a certain certain external pressure drop and power there is only possible steady state mass flux, thus making a Ledinegg instability impossible.

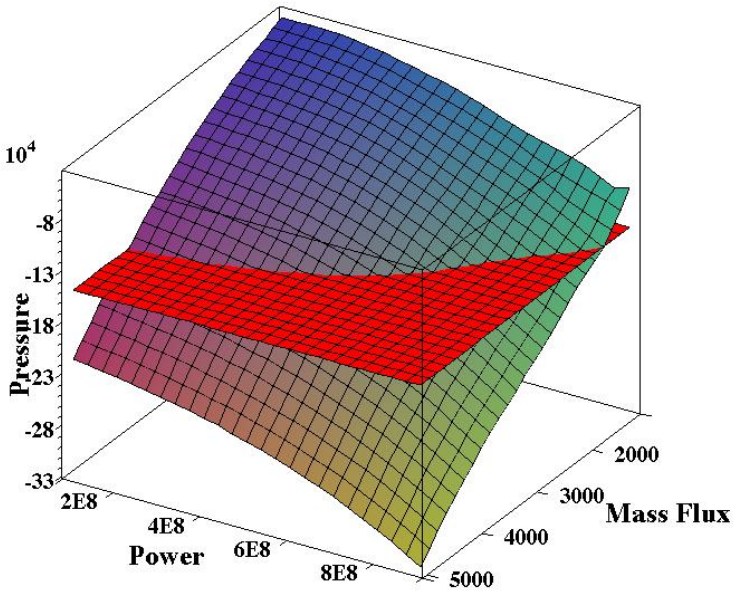

Figure C.1: Given a certain power and pressure drop there is only one possible mass flux.

Appendix D

Steady State Solver

Contents


```
% Kin 1-pass Kout
%%%%%%%%%%%%%%%%%%%%%%%%%%%%%%%%%%%%%%%%%%%%%%%%%%%%%%%%%%%%%%%%%%%%%%%%%%%%%%%%
%%%%%%%%%%%%%%%%%%%%%%%%%%%%%%%%%%%%%%%%%%%%%%%%%%%%%%%%%%%%%%%%%%%%%%%%%%%%%%%%
% Createrd by Maarten Sanders
% based on code devoloped by Tino Ortega-Gomez
% TU Delft
% Radioactivity, Radionuclides and Reactors
% Physics of Nuclear Reactors
% 28-04-09
% This program simulates the single pass core concept for a Super Critical
% Water Reactor, with inlet and outlet valves at the beginnning and the end
% of the core.
%%%%%%%%%%%%%%%%%%%%%%%%%%%%%%%%%%%%%%%%%%%%%%%%%%%%%%%%%%%%%%%%%%%%%%%%%%%%%%%%
%%%%%%%%%%%%%%%%%%%%%%%%%%%%%%%%%%%%%%%%%%%%%%%%%%%%%%%%%%%%%%%%%%%%%%%%%%%%%%%%

clear

flclear fem %clean up
```

```
% Femlab version
clear vrsn
vrsn.name = 'FEMLAB 3.1';
vrsn.ext = '';
vrsn.major = 0;
vrsn.build = 157;
vrsn.rcs = '$Name:  $';
vrsn.date = '$Date: 2004/11/12 07:39:54 $';
fem.version = vrsn;
```

Constants

standard SI units are used

```
fem.const={...
    'Hin','0',...     % inlet enthalpy (boundary condition) T=310C
    'geff','9.81',... % effective acceleration due gravity
    'Dhydr','0',...   % hydraulic diameter of the flow channel old hplwr 0.006839
    'Pdrop','0',...   % channel‘s pressure drop (boundary condition) 155.38 of 28.7
    'Gin','1780',...  % Inlet mass flux (just needed for initial value)
    'qw','0',...      %1.967 effective uniform heat flux q/L = 30kW/m
    'Pin','0.001',...               % inlet pressure (only for initial value)
    'Kin','0',...                   % inlet loss coefficient
    'Kout','0',...                  % exit loss coefficient
    'scale','1',...                 % scales all friction effect
    'roughness','0',...% sets the roughness of the channel (important for wall frict
    'Lcore','0'};                   % initialised here but set further on
```

Governing Equations

Subdomain expressions

```
clear equ   % clean up

equ.ind = [1];
equ.dim = {'H','P','G'};
equ.expr = {...
        'friction','1/(-1.8*log10((roughness/Dhydr/3.7)^1.11+6.9/Re_1))^2',...
                                        % Darcy Wei?bach friction factor relatio
        'cfric','friction/(2*Dhydr)',...    % Wall friction
        'Nfr', '(G/rho)^2/(Lcore*geff)',... % Froude number
        'Nphase', 'qw/G/Dhydr^2/290261',... % Pseudo-phasechange number
        'Re_1','abs(G*Dhydr/mu)',...        % Reynolds number
```

```
        'F1','v*qw-G*v*Hx',...              % Energy conservation equation
        'F2','-(geff/v+G*G*v*cfric+Px)',... % Momentum conservation equation
        'F3','Gx*v*v/DvDH',...              % Mass conservation equation
        'DvDH','-DrhoDH/(rho*rho)',...      % derivation to the enthalpy of specific
        'vin','1/rhoin',...                 % specific volume at inlet
        'v','1/rho'};                       % specific volume
```

Setting fluid specific properties

```
%Scaling laws:
Gwater = 6858;
X_h = 0.134;
X_rho = 1.691;
Dhyd = 0.00562;%std 0.00562
rough = 4e-7;
Power = 8e8;
Hin = 1.4e6;

button = questdlg('Which fluid do you want to simulate, water or freon?: ',...
    'Choice of Fluid','Water','Scaled Water','Freon (R23)','Scaled Water');
switch button
    case 'Scaled Water'
        liquid = 'Freon';
        name = 'scaled_water'
        equ.expr{end+1}= 'rho';
        equ.expr{end+1}= '+(-2.11959e-014*(H-107202)^{3}..... [rest of density splin
        equ.expr{end+1}= 'rhoin';
        equ.expr{end+1}= '+(-2.11959e-014*(Hin-107202)^3....[rest of spline follows]
        equ.expr{end+1}= 'DrhoDH';
        equ.expr{end+1}= '+(-8.19981e-019*(H-107202)^3.......[rest of spline follows
        equ.expr{end+1}= 'mu';
        equ.expr{end+1}= '+(-4.54737e-020*(H-107202)^3.......[rest of spline follows
        %equ.expr{end+1}= '-1.541e-021*H^3 + 2.579e-015*H^2 + -1.321e-009*H+ 0.00023

    case 'Water',
            L = 4.2;
        liquid = 'Water';
        name = 'Water'
        fem.const(2) = cellstr(sprintf('%d',Hin));
        fem.const(24) = cellstr(sprintf('%d',L));
        fem.const{8} = '-300e3';     % Pdrop ref is -135.67kPa
        fem.const(6) = cellstr(sprintf('%d',Dhyd));
        fem.const(12) = cellstr(sprintf('%d',Power));
        fem.const(22) = cellstr(sprintf('%d',rough));
```

```
        equ.expr{end+1}= 'rho';
        equ.expr{end+1}= '+(-2.9416e-17*(H-800000)^3....[rest of spline follows]
        equ.expr{end+1}= 'rhoin';
        equ.expr{end+1}='+(-2.9416e-17*(Hin-800000)^3....[rest of spline follows]
        equ.expr{end+1}= 'DrhoDH';
        equ.expr{end+1}=  '+(-3.01126e-21*(H-1e+06)^3.....[rest of spline follows]
        equ.expr{end+1}= 'mu';
        equ.expr{end+1}='+(-1.33219e-22*(H-800000)^3.....[rest of spline follows]

   case 'Freon (R23)',
        liquid = 'Freon';
        name = 'freon'
        % These are the real R23 splines
        equ.expr{end+1}= 'rho';
        equ.expr{end+1}= '+(-2.73706e-14*(H-107200)^3.....[rest of spline follows]
        equ.expr{end+1}= 'DrhoDH';
        equ.expr{end+1}= '+(1.82323e-18*(H-107200)^3....[rest of spline follows]
        equ.expr{end+1}= 'mu';
        equ.expr{end+1}= '+(-4.54737e-020*(H-107202)^3....[rest of spline follows]
end

if liquid=='Freon'
button = questdlg('Which geometry do you want to simulate?: ',...
        'Geometry','Ideal Scaling','Ideal Setup','Actual Setup','Ideal Setup');
    switch button
        case 'Ideal Scaling'
            L = 2.592;
            X_G = 1.329;
            fem.const{8} = '-300e3';     % scaled water 141.4, freon is 141.7
            X_qw = 0.288;
            X_Dh = 0.617;
            X_rough = X_Dh;

        case 'Ideal Setup',
            L = 0.804;
            X_Dh = 1.063;
            X_G = 0.740;
            X_qw = 0.518;
            X_rough = 1;
            switch name
                %The pressure drop is set here. Though the difference
                %between  small to achieve the same mass flux and have a
                %converging solution.
                case 'freon'
```

```
                    fem.const{8} = '-20.2e3';
                case 'scaled_water'
                    fem.const{8} = '-20635';
                otherwise
                    fprintf('name not recognised.\r')
            end

        case 'Actual Setup',
            L = 0.8;
            X_G = 0.740;
            X_Dh = 0.006/Dhyd;
            X_qw=0.518;
            X_rough = 1;
            switch name
                case 'freon'
                    fem.const{8} = '-20.1e3';
                case 'scaled_water'
                    fem.const{8} = '-20.6e3';
                otherwise
                    fprintf('name not recognised.\r')
            end

        otherwise
            fprintf('liquid not recognised.\r')
            break
    end
    fem.const(2) = cellstr(sprintf('%d',Hin*X_h));
    fem.const(24) = cellstr(sprintf('%d',L));
    fem.const(10) = cellstr(sprintf('%d',Gwater*X_G));    % Gin
    fem.const(6) = cellstr(sprintf('%d',Dhyd*X_Dh));
    fem.const(12) = cellstr(sprintf('%d',Power*X_qw));
    fem.const(22) = cellstr(sprintf('%d',rough*X_rough));

end


fem.equ = equ;
temp = equ.expr; %saving equ.expr to be used later on to prevent double definitions
```

```
Error: A BREAK statement appeared outside of a loop. Use RETURN instead.
```

Geometry

```
g1=solid1([-0.175,L+0.175]); %1D solid line for 4.2m lenght
```

```
% NOTE that changing the length of the inlet and outlet sections also means
% changing the way they are implemented in 'friction'!!!
clear s
s.objs={g1};
s.name={'I1'};
s.tags={'g1'};

fem.draw=struct('s',s);
fem.geom=geomcsg(fem);
tic
```

BC's & IC's

Application mode 1

```
clear appl                                          % clean up
appl.mode.class = 'FlPDEG';                         % Partial Differential Equation mode
appl.dim = {'H','P','G','H_t','P_t','G_t'};         % state variables: H = Enthalpy (not
appl.shape = {'shlag(5,''H'')','shlag(4,''P'')','shlag(5,''G'')'}; %shape-functions
appl.gporder = 10;
appl.cporder = 5;
appl.assignsuffix = '_g';
clear bnd                                           % clean up
bnd.weak = {{1;1},{0;1}};                           % weak boundary definition
bnd.r = {{'-H+Hin';'-P+G*G*vin'},{0;'-P+Pdrop+G*G*v'}}; % boundary condition: actual
bnd.ind = [1,2];                                    % boundary definition             %
appl.bnd = bnd;
clear equ                                            % clean up
equ.init = {{'Hin';'Pin+Gin*Gin*vin';'Gin';0;0;0}}; % init values
equ.weak = {{'H_test*F1';'P_test*F2';'G_test*F3'}}; % weak form for good convergence
equ.dweak = {{'H_time*H_test';'G_time*P_test';'H_time*G_test'}}; % weak form for goo
equ.da = {{1,0,0;0,0,1;1,0,0}};                        % time derivatives. Note: da mus
equ.f = {{'F1';'F2';'F3'}};                            % ride hand side of conservation
equ.ga = 0;                                            % note above: mass conservation
equ.ind = [1];
appl.equ = equ;
fem.appl{1} = appl;
fem.border = 1;
fem.outform = 'weak';                                  % weak form

% Multiphysics
fem=multiphysics(fem);

% Initialize mesh
```

```
%fem.mesh=meshinit(fem);

 coremesh = L/10;
 fem.mesh=meshinit(fem, ...
    'hmax',[coremesh]);

% Extend mesh
fem.xmesh=meshextend(fem, ...
    'linshape',[]);
```

First Solution

Solve problem

```
fem.sol=femstatic(fem, ...
    'solcomp',{'G','P','H'}, ...
    'outcomp',{'G','P','H'}, ...
    'hnlin','on');

% Save current fem structure for restart purposes
fem0=fem;
toc
```

Geometry 2

```
g2=point1(0);
g3=point1(L);

% Analyzed geometry
clear p s
p.objs={g2,g3};
p.name={'PT1','PT2'};
p.tags={'g2','g3'};

s.objs={g1};
s.name={'I1'};
s.tags={'g1'};

fem.draw=struct('p',p,'s',s);
fem.geom=geomcsg(fem);

% (Default values are not included)
```

Application mode 2

```
clear bnd
bnd.r = {{'-H+Hin';'-P+G*G*vin'},{0;'-P+Pdrop+G*G*v'}, ...
  {'-H';'-P';'-G'}};
bnd.weak = {{1;1},{0;1},0};
bnd.type = {'dir','dir','neu'};
bnd.ind = [1,3,3,2];
appl.bnd = bnd;
clear equ
equ.f = {{'F1';'F2';'F3'}};
equ.da = {{1,0,0;0,0,1;1,0,0}};
equ.dweak = {{'H_time*H_test';'G_time*P_test';'H_time*G_test'}};
equ.init = {{'Hin';'Pin+Gin*Gin*vin';'Gin';0;0;0}};
equ.ga = 0;
equ.weak = {{'H_test*F1';'P_test*F2';'G_test*F3'}};
equ.ind = [1,1,1];
appl.equ = equ;
fem.appl{1} = appl;
fem.border = 1;
fem.outform = 'weak';

% Subdomain settings
clear equ
equ.ind = [1,2,3];
equ.dim = {'H','P','G'};

% Subdomain expressions
equ.expr = temp;
equ.expr;
equ.expr{2} ={'Kin/0.175','1/(-1.8*log10((roughness/Dhydr/3.7)^1.11+6.9/Re_1))^2','
equ.expr{4} = {'scale*0.5*friction','scale*0.5*friction/Dhydr','scale*0.5*friction'
equ.expr{12} = {'v*(-G*Hx)','v*(qw-G*Hx)','v*(-G*Hx)'};
equ.expr{14} ={'-G^2*v*cfric-Px','-geff/v-G^2*v*cfric-Px','-G^2*v*cfric-Px'};
fem.equ = equ;
```

Setting Mesh Parameters

Initialize mesh

```
coremesh = L/480;
inlet = 0.0175;
fem.mesh=meshinit(fem, ...
    'hmaxsub',[1,inlet,2,coremesh,3,inlet]);
```

```
% Multiphysics
fem=multiphysics(fem);

% Extend mesh
fem.xmesh=meshextend(fem, ...
    'linshape',[]);

% Mapping current solution to extended mesh
init = asseminit(fem,'init',fem0.sol,'xmesh',fem0.xmesh);
u = init;
```

Second Solution

Solve problem

```
fem.sol=femstatic(fem, ...
    'init',init, ...
    'u',u, ...
    'solcomp',{'G','P','H'}, ...
    'outcomp',{'G','P','H'}, ...
    'hnlin','on');

% Save current fem structure for restart purposes
fem0=fem;

save(name)
toc
```

Appendix E

NSB Calculation Code

```
%%%%%%%%%%%%%%%%%%%%%%%%%%%%%%%%%%%%%%%%%%%%%%%%%%%%%%%%%%%%%%%%%%%%%%%%%%%%
% This program requires a predifined system as input. This must be in the
% fem format used by COMSOL and include information on the liquid. The file
% HPLWR_v4 will produce the correct output which is named either water.mat,
% freon.mat or scaled_water.mat . The program then defines a starting
% point for which the st.st. is calculated. The heating power is then
% increased untill the NSB is crossed after which the program makes an
% educated guess as to the location of the NSB. Once the NSB has been
% crossed the program will usually find it within 1 to 2 iterations. Once
% the correct st.st. has been found the dimensionless numbers are stored and
% the inlet enthalpy is increased. The program can also execute a
% parameter study which is basically a number of NSB investigations done
% one after the other.
% The different data are stored as follows:
%   Npch_sc = dimensionless enthalpy jump number
%   Nsub_sc = subcooling number
%   Npch_para3 = psuedo-phasechange number
%   Nsub_para3 = pseudo-subcooling number
% For definitions of these numbers see Msc thesis Maarten Sanders on HPLWR
% stability.
%%%%%%%%%%%%%%%%%%%%%%%%%%%%%%%%%%%%%%%%%%%%%%%%%%%%%%%%%%%%%%%%%%%%%%%%%%%%

clear

prog = input('Which starting file (.mat) do you want to use?','s');
para3str = input('Which parameter do you want to investigate (k-in,kout,pdrp,scal o
para3 = input('Which values of the parameter do you want to investigate?');
tic
load(prog)
```

```
if liquid == 'Water'
    %Setting values of Hin to be calculated
    paraN1 = 7;
    para1initial = 1.3e6;   %std is 1.1e6
    para1final = 1.9e6;     %std is 1.9 e6
    para1 = linspace(para1initial,para1final,paraN1);
    %Defining Initial Scan
    qw = 8e8;
    qwstep = 1e8;
elseif liquid == 'Freon'
    %Setting values of Hin to be calculated
    paraN1 = 8;
    X_h = 0.134;
    para1initial = X_h*1.2e6;
    para1final = X_h*1.9e6;
    para1 = linspace(para1initial,para1final,paraN1);
    %Defining Initial Scan
    qw =sscanf(fem.const{12},'%g');
    qwstep = 0.5e8;
end

fem.const(12) = cellstr(sprintf('%d',qw));
paraN3 = length(para3);

%Pre-allocating matrices to improve calculation speed
eig_Hin = zeros(1,paraN1);
Npch_Hin = zeros(1,paraN1);
Nsub_Hin = zeros(1,paraN1);
qw_Hin = zeros(1,paraN1);

Npchpara3 = zeros(paraN3,paraN1);
Nsubpara3 = zeros(paraN3,paraN1);
qwpara3 = zeros(paraN3,paraN1);
Nsub_sc = zeros(paraN3,paraN1);
Npch_sc = zeros(paraN3,paraN1);
eigpara3 =zeros(paraN3,paraN1);

sol(1) = fem;

if para3str =='k-in'
    para3num = 16;
elseif para3str == 'kout'
    para3num = 18;
```

```
elseif para3str == 'pdrp'
      para3num = 8;
elseif para3str =='scal'
    para3num = 20;
elseif para3str =='dhyd'
    para3num = 6;
elseif para3str =='epsi'
    para3num = 22;
else
    fprintf('wrong parameter entered')
    break
end

% Location within fem.const of parameters:
% Hin is at 2
% geff is at 4
% Dhydraulic is at 6
% Pdrop 8
% Gin 10 (not usefull to change)
% qw 12
% Pin 14 (not usefull to change)
% Kin 16
% Kout 18
% scale 20


for k = 1:paraN3 %Loop varying the parameter under investigation
    fem = sol(k);
    fem0=fem;
    init=fem;
    fem.const(para3num) = cellstr(sprintf('%d',para3(k)));
    fprintf('%s = %g\r',para3str,para3(k))

    for i = 1:paraN1 %Loop varying the inlet enthalpy

        clear eig eig_old

        %Calculating initial st.st.
        fem.const(2) = cellstr(sprintf('%d',para1(i)));
        fprintf('Inlet enthalpy = %g \r',para1(i));
        solve_stst %subroutine which solves the steady state problem

        %Solving for eigenvalues
        solve_eig %subprogram which uses the current steady state solution to the ei
```

```
eig_old = eig;
eig1 = eig

%Find the first unstable workingpoint by calculating the
%eigenvalues of st.st.'s. Once the sign of the eigenvalues changes
%the neutral stability boundary (NSB has been crossed), after which
%a more intelligent manner of finding the NSB can be used (next
%'while' loop).
while sign(eig_old)==sign(eig)
    qw_old = qw;
    if i == 1 %larger steps are used to find the initial neutral stability p
        qw = qw + sign(eig)* qwstep;
    else
        qw = qw + sign(eig)* qwstep/2;
    end
    fem.const(12) = cellstr(sprintf('%d',qw));%changing the heating power
    fprintf('Power = %g\r',qw)
    solve_stst
    eig_old = eig;
    solve_eig
    eig1 = [eig1 eig];
    eig
    if qw >2e9 %once the power exceeds this number it is unlikely that the N
        fprintf('Hmmmmmm....qw is now larger than 20e8')
        break
    elseif qw<1e7 %minimum heating power, lower powers are unlikely
        fprintf('hmmmmm_v2...qw is now smaller than 1e8')
        break
    end
end

accuracy = 0.02;
%Checking whether the inital guess is exactly on the NSB
if eig<-accuracy
    stable = qw_old;
    eigstable = eig_old;
elseif eig>accuracy
    unstable = qw_old;
    eigunstab = eig_old;
elseif abs(eig)<accuracy %guess is exactly on NSB and dimensionless numbers
    solve_stst
    calc_dimnum %calcuates the dimensionless numbers (Tino's and Martin's) a
end
```

```
j = 0;

while abs(eig)>accuracy
    j=j+1; %counter; if it exceeds 8 a solution is not likely to be found ar

    %Making an educated guess of the location of the NSB. The NSB
    %is usually found within 1 or 2 iterations.
    if eig>0
        stable = qw;
        eigstable = eig;
        qw = stable + eigstable/(eigstable-eigunstab)*(unstable-stable);
    elseif eig<0
        unstable = qw;
        eigunstab = eig;
        qw = unstable + eigunstab/(eigstable-eigunstab)*(unstable-stable);
    else
        fprintf('error.... tja wat nu?')
    end

    %ends calculation if this is the 8th iteration
    if j==8
        fprintf('%g\r',eig)
        fprintf('%g\r',eig_old)
        fprintf('%g\r',qw)
        fprintf('Neutral stability point cannot be found \r')
        load chirp
        sound(y,Fs)
        break
    end

    fprintf('Power = %g\r', qw)

    %prints the power which has just been calculated using an
    %educated guess
    fem.const(12) = cellstr(sprintf('%d',qw));
    fem.const(12);

    solve_stst
    %st.st. solution needs to be save since we only know if it is
    %the correct one once the eigenvalue calculation has been made.
    if i==1
        sol(k+1)=fem;
    end
    calc_dimnum
```

```
            solve_eig
        end

        Power = qw;

        Nsub_sc(k,i) = Nsub_scale;
        Npch_sc(k,i) = Npch_scale;
        Npchpara3(k,i) = Npch;
        Nsubpara3(k,i) = Nsub;
        qwpara3(k,i) = qw;
        eigpara3(k,i) = eig;
    end
    toc
end

%Saving the (minimum) essential information
save(sprintf('Neutral %s %1.2g tot %1.2g.mat',para3str,para3(1),para3(k))...
    ,'qwpara3','Nsubpara3','Npchpara3','para3','para1','eigpara3','fem',...
    'Nsub_sc','Npch_sc')

%sound to signal that the program has finished (fun to play with)
load handel
sound(y(1:20000)./15,Fs*1.2)
toc


Error: A BREAK statement appeared outside of a loop. Use RETURN instead.
```

List of Figures

List of Tables